J Neurophysiol 90: 415–430, 2003.
First published February 26, 2003; 10.1152/jn.01095.2002.

What Determines the Frequency of Fast Network Oscillations With Irregular Neural Discharges? I. Synaptic Dynamics and Excitation-Inhibition Balance

Nicolas Brunel[1] and Xiao-Jing Wang[2]

[1]*Centre National de la Recherche Scientifique-Neurophysique et Physiologie du Système Moteur-Université Paris René Descartes, 75270 Paris Cedex 06, France; and* [2]*Volen Center, Brandeis University, Waltham, Massachusetts 02454*

Submitted 6 December 2002; accepted in final form 11 February 2003

Brunel, Nicolas and Xiao-Jing Wang. What determines the frequency of fast network oscillations with irregular neural discharges? I. Synaptic dynamics and excitation-inhibition balance. *J Neurophysiol* 90: 415–430, 2003. First published February 26, 2003; 10.1152/jn.01095.2002. When the local field potential of a cortical network displays coherent fast oscillations (~40-Hz gamma or ~200-Hz sharp-wave ripples), the spike trains of constituent neurons are typically irregular and sparse. The dichotomy between rhythmic local field and stochastic spike trains presents a challenge to the theory of brain rhythms in the framework of coupled oscillators. Previous studies have shown that when noise is large and recurrent inhibition is strong, a coherent network rhythm can be generated while single neurons fire intermittently at low rates compared to the frequency of the oscillation. However, these studies used too simplified synaptic kinetics to allow quantitative predictions of the population rhythmic frequency. Here we show how to derive quantitatively the coherent oscillation frequency for a randomly connected network of leaky integrate-and-fire neurons with realistic synaptic parameters. In a noise-dominated interneuronal network, the oscillation frequency depends much more on the shortest synaptic time constants (delay and rise time) than on the longer synaptic decay time, and ~200-Hz frequency can be realized with synaptic time constants taken from slice data. In a network composed of both interneurons and excitatory cells, the rhythmogenesis is a compromise between two scenarios: the fast purely interneuronal mechanism, and the slower feedback mechanism (relying on the excitatory-inhibitory loop). The properties of the rhythm are determined essentially by the ratio of time scales of excitatory and inhibitory currents and by the balance between the mean recurrent excitation and inhibition. Faster excitation than inhibition, or a higher excitation/inhibition ratio, favors the feedback loop and a much slower oscillation (typically in the gamma range).

INTRODUCTION

Fast network oscillations (from 40 to 200 Hz) have been recorded in vivo in several brain areas. In particular, the rat hippocampus displays prominent gamma (40–80 Hz) rhythm during animal's free movement and rapid-eye movement (REM) sleep, and 200-Hz sharp-wave ripples during quiet sleep and immobility as measured by local field potential (LFP) (Bragin et al. 1995; Buzsaki et al. 1992; Csicsvari et al. 1999b; Siapas and Wilson 1998). Single-cell discharge rates is typically much lower than the LFP oscillation frequency, especially in pyramidal cells but also in interneurons (Csicsvari et al. 1998, 1999b). Indeed rhythmicity is usually not apparent in the raw spike trains of individual cells and becomes visible only after data processing of spike trains from multiple single units. Thus single-cell behavior differs markedly from the population activity during fast network oscillations. Similarly, physiological studies of primates indicate that even when the LFP signal contains a clear rhythmic component, simultaneously recorded single-unit spike trains usually appear irregular and devoid of a clear-cut oscillation (Fries et al. 2001; Logothetis et al. 2001).

Recently, oscillations have been observed in vitro (Buhl et al. 1998; Fellous and Sejnowski 2000; Fisahn et al. 1998) that resemble these characteristics: strong gamma (30–40 Hz) oscillation of the LFP, together with low (<2 Hz) and irregular firing in pyramidal cells. This means that a single pyramidal cell fires only once in every 15–20 cycles of the population rhythm. Fast rhythmic ripples at 100–200 Hz have also been produced in hippocampal slices, again with intermittent principal cell firing (Draguhn et al. 1998). The observations in the slices of rhythmic activity patterns at high frequencies have opened a promising venue to study the underlying cellular and circuit mechanisms.

Computational models of networks of spiking neurons have shown how synchrony could emerge in recurrent networks of interneurons. However, in models with weak synaptic disorder and weak noise, neurons behave typically as oscillators and fire at network frequency (see e.g., Abbott and van Vreeswijk 1993; Gerstner 1995; Gerstner et al. 1996; Hansel et al. 1995; Kopell and Ermentrout 1986; Kuramoto 1984; Marder 1998; Traub et al. 1996; Treves 1993; Wang and Buzsáki 1996). In some cases, modes of synchrony called "clustering" occur in which the network breaks in a small number of fixed clusters of neurons. In these cases, the network frequency is higher than the frequency of single cells, being equal to the number of clusters times the frequency of single cells, but single cells still fire in a regular fashion (Golomb and Rinzel 1994; Kopell and LeMasson 1994; Wang et al. 1995). Heterogeneities tend to disrupt synchrony; but in parameter ranges for which synchrony is present, the network oscillation is not qualitatively affected by heterogeneity: neurons keep firing in a regular fashion and the network frequency is close to the average frequency of the cells of the network (or an integer multiple in case of clustering) (Bartos et al. 2001; Golomb and Hansel

Address for reprint requests: N. Brunel, CNRS-NPSM-Université Paris René Descartes, 45 rue des Saints Pères 75270 Paris Cedex 06, France (E-mail: brunel@biomedicale.univ-paris5.fr).

The costs of publication of this article were defrayed in part by the payment of page charges. The article must therefore be hereby marked "*advertisement*" in accordance with 18 U.S.C. Section 1734 solely to indicate this fact.

2000; Hansel and Mato 2001; Wang and Buzsáki 1996; White et al. 1998). In contrast to the framework of coupled oscillators, several studies (Brunel and Hakim 1999; Brunel 2000; Tiesinga and Jose 2000) have shown that a network oscillation can be produced with low and intermittent spike discharges in pyramidal cells and interneurons under conditions of strong noise (in external inputs and/or due to disorder in recurrent connectivity) and strong recurrent inhibition. However, Brunel and Hakim (1999) and Brunel (2000) used too-simplified synaptic currents to draw quantitative conclusions about oscillation frequencies in real networks, and Tiesinga and Jose (2000) used a purely numerical approach, making it difficult to identify the crucial parameters controlling network frequency. More recently, several studies (Lewis and Rinzel 2000; Schmitz et al. 2001; Traub et al. 1999; Traub and Bibbig 2000) have suggested that 200-Hz oscillations with sparse pyramidal firing could be realized by gap junctions between axons of pyramidal cells. However, 200-Hz oscillations in a slice preparation are not affected in transgenetic mice with knockout of the gap-junction protein connexin 36 (Buhl et al 2003; Hormuzdi et al. 2001). The possibility remains that other subtypes of gap-junction proteins different from connexin 36 play the hypothesized role in rhythmogenesis (Schmitz et al. 2001). Connexin 36-deficient mice shows gamma oscillations at the same frequency as the control but with a reduced level of population synchrony (Buhl et al 2003; Hormuzdi et al. 2001). Therefore it is still unclear whether the *frequency* of fast network oscillations in hippocampus critically depends on the gap junctions.

When single neurons do not fire in a periodic fashion but rather fire stochastically at low rates, several questions remain unanswered: what determines the frequency of fast oscillations with sparsely firing neurons in networks with realistic neuronal and synaptic properties? Can such high frequencies as are observed in vivo be generated by chemical synapses and in the absence of gap junctions? To shed light onto these questions, we have analyzed coherent population oscillations, characterized by sparse and irregular firing of single cells, in a recurrent network model with realistic synaptic time courses. In this paper, we present an analytical approach to predict the population oscillation frequency from synaptic and network parameters in such a recurrent neural network. This approach allows to identify the requirements on the synaptic circuitry under which fast gamma and ripple rhythmicities occur in the sparsely firing regime.

METHODS

Neurons

Both interneurons and pyramidal cells are described as leaky integrate-and-fire (LIF) neurons (see e.g., Tuckwell 1988), with membrane time constants $\tau_m = 20$ ms (pyramids) and 10 ms (interneurons). The leak (resting) membrane potential is -70 mV, the spike threshold is -52 mV, and the reset potential is -59 mV. The absolute refractory period is 2 ms (pyramids) and 1 ms (interneurons).

Networks

The network architecture is random and sparse, with a given connection probability. We used three types of networks: networks of N_I interneurons only, with random interneuron-interneuron connections; networks of N_I interneurons and N_E pyramidal cells, with random interneuron-interneuron, interneuron-pyramid, and pyramid-interneuron connections (i.e., without pyramid-pyramid connections); and networks of N_I interneurons and N_E pyramidal cells, with all four possible connections, drawn randomly with the same connection probability. In simulations, we used typically $N_I = 1{,}000$, $N_E = 4{,}000$. The connection probability p between any pair of cells was typically 20%. Thus each cell in the network received ~200 synaptic contacts from other interneurons and ~800 from pyramidal cells.

Synaptic currents

Three types of synaptic currents were used, modelling GABAergic (inhibitory), AMPA-type (fast excitatory) and *N*-methyl-D-aspartate (NMDA)-type (slow excitatory) synaptic inputs. The synaptic currents were described as $I_{syn}(t) = g_{syn}(V - V_{syn})s(t)$ where g_{syn} is the synaptic conductance, V_{syn} the corresponding reversal potential, and $s(t)$ is a function describing the time course of synaptic currents. We used a delayed difference of exponentials: if a presynaptic spike occurs at time 0, then after a latency τ_l, $s(t)$ is updated as

$$s(t) = \frac{\tau_m}{\tau_d - \tau_r}\left[\exp\left(-\frac{t-\tau_l}{\tau_d}\right) - \exp\left(-\frac{t-\tau_l}{\tau_r}\right)\right]$$

where the normalization constant is chosen so that the time integral of $s(t)$ is equal to the membrane time constant τ_m. This normalization was chosen so that varying the synaptic time constant does not affect the time integral of a postsynaptic current (PSC). The peak of the function s is

$$s_{peak} = \frac{\tau_m}{\tau_d}\left(\frac{\tau_r}{\tau_d}\right)^{\frac{\tau_r}{\tau_d - \tau_r}}$$

Therefore the synaptic kinetics is defined with three parameters: latency τ_l, rise time τ_r, and decay time τ_d. The reversal potential of excitatory (inhibitory) synaptic currents is 0 mV (-70 mV). Synaptic conductances were calibrated such as the amplitude of PSCs was in the range of 0.2–2 mV at holding potential of -55 mV, i.e., just below threshold, in accordance with slice data (Buhl et al. 1997; Markram et al. 1997; Tamas et al. 1997, 1998; Vida et al. 1998). They yielded peak conductances, for AMPA receptors, ~1 nS; for NMDA receptors, ~0.01 nS; for GABA receptors, ~6 nS, compatible with experimentally inferred values (Bartos et al. 2001, 2002; Gupta et al. 2000; Markram et al. 1997). See Table 1 for more details on parameters.

All synaptic time scales were systematically varied, but typical "reference" parameters were, for GABAergic currents, $\tau_l = 1$ ms, $\tau_r = 0.5$ ms, and $\tau_d = 5$ ms (Bartos et al. 2001; Gupta et al. 2000; Kraushaar and Jonas 2000; Xiang et al. 1998); for AMPA currents, $\tau_l = 1$ ms, $\tau_r = 0.5$ ms, and $\tau_d = 2$ ms (Angulo et al. 1999; Zhou and Hablitz 1998); for NMDA currents, $\tau_l = 1$ ms, $\tau_r = 2$ ms, and $\tau_d = 100$ ms (Hestrin et al. 1990). NMDA conductances could be removed from all simulations without affecting any of the results.

The equivalence between g parameters, peak conductances, ampli-

TABLE 1. *Synaptic model parameters*

	g_{syn}, nS	Peak conductance = $g_{syn}s_{peak}$, nS	PSC amplitude, pA	PSP amplitude, mV
AMPA on pyramids	0.19	1.18	65	0.32
AMPA on interneurons	0.3	0.95	52	0.54
GABA on pyramids	2.5	7.75	116	0.9
GABA on interneurons	4	6.2	93	1.4
NMDA on pyramids	0.06	0.012	0.6	0.02
NMDA on interneurons	0.1	0.009	0.5	0.02

Sum of s variables over all excitatory (inhibitory) synapses is denoted in the following by $s_E(s_I)$. PSC and PSP, postsynaptic current and potential; NMDA, *N*-methyl-D-aspartate.

tude of PSCs at −55 mV, and amplitude of PSPs at −55 mV are given (for the reference synaptic time scales) in the table.

External inputs

External inputs were assumed to arise from 800 external synapses of the AMPA type, with conductance 0.25 nS (on pyramids), 0.4 nS (on interneurons), and the same kinetics as recurrent AMPA synapses. The synapses are activated by random Poisson spike trains, with a given rate. In RESULTS, we mention the total input Poisson rate for each simulation shown.

Numerical methods

Simulations were done using a finite difference integration scheme based on the second-order Runge Kutta algorithm (Hansel et al. 1998; Press et al. 1992; Shelley and Tao 2001) with time step $dt = 0.05$ ms. Shorter time steps did not change the results in any significant way. Typical simulation times were carried out for 10 s of real time. Simulations were run on workstations with alpha architecture and lasted of the order of one hour. We used two types of synchrony indices.

SPIKE TRAIN SYNCHRONY (STS) INDEX. We compute the autocorrelation of total network activity, computed in bins of 1 ms. The autocorrelation is normalized by the square of the average firing rate of cells in the network. The spike train synchrony index is defined as the autocorrelation at zero time. Its intuitive interpretation is the following: if the index is one, it means the chance that two randomly selected neurons fire together in a 1-ms bin is 100% higher than if these neurons were firing in an uncorrelated way. The frequency of the oscillation was determined from the peak of the power spectrum of the global activity.

MEMBRANE POTENTIAL SYNCHRONY (MPS) INDEX. Average correlation between the membrane potentials of two neurons in the network, normalized to 1 when all membrane potentials have the same time course (Hansel and Sompolinsky 1996).

The advantage of the first index is that it is directly related to measurable quantities in vivo such as cross-correlations between spike trains (it is equal to the CC at 0 time, averaged over pairs). The advantage of the second is that it is bounded between 0 and 1. In all simulations series, we found, unsurprisingly, that both indices behave qualitatively in a very similar way.

Synchrony indices are always nonzero in simulated networks due to finite size effects (Brunel and Hakim 1999; Hansel and Sompolinsky 1996; Wang and Buzsáki 1996). To determine whether the network is in an asynchronous or synchronous state, we performed simulations with varying network sizes, keeping the number of connections and the synaptic conductance fixed so as to keep unchanged the temporal average and fluctuations of the synaptic currents as network size was varied. In an asynchronous state, the synchrony indices strongly decrease and go to zero with increasing N. In a synchronous state, the synchrony index decreases only mildly and tends to a finite value in the large N limit. An alternative strategy for finite size scaling has been proposed by Golomb and Hansel (2000). Both approaches are expected to give the same results in the limit in which connection probability becomes small.

RESULTS

Oscillations in a network of purely inhibitory neurons

Figure 1 shows the behavior of a simulated interneuronal network. A pronounced population activity oscillation is clearly visible at a frequency of ~180 Hz. On the other hand, the single cell activity reveals a much lower activity (average of ~20 spikes/s), with a wide range of individual firing rates

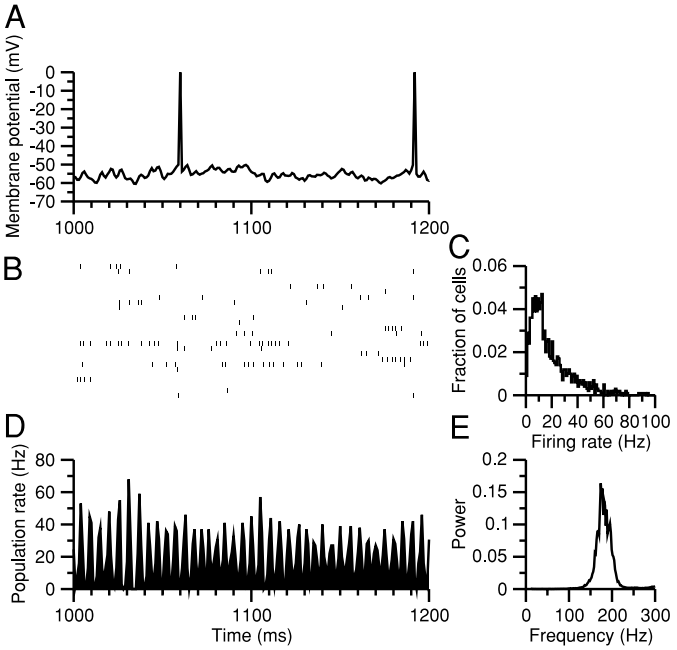

FIG. 1. Synchronous network oscillation (at 180 Hz), where single neurons fire spikes sparsely and irregularly, in a network of inhibitory integrate-and-fire neurons. *A*: membrane potential of a single neuron. The average total currents are subthreshold, and the neuron fires only due to occasional fluctuations that bring it above threshold. Weak subthreshold membrane oscillations can be seen in correspondence with global activity fluctuations. *B*: rastergram shows low-rate and irregular spike trains from individual neurons. The neuron in *A* is the neuron shown at the bottom of the rastergram. *C*: distribution of single neuron's firing rate across the population shows a wide range of rates from 0 to 100 Hz. *D*: instantaneous population firing rate displays pronounced rhythmicity at ~180 Hz, as clearly seen in its power spectrum (*E*). The network has 1,000 cells, the architecture is random with connection probability of 0.2. External input rate 12 kHz; GABAergic synapses with latency 1 ms, rise time 0.5 ms, decay time 5 ms.

(from 0 to 100), and the spiking process is highly irregular. Thus in any cycle of the oscillation, only ~10% of the interneurons actually fire. The intuitive explanation for the oscillatory phenomenon is the following: single neurons receive a strong inhibitory drive due to powerful recurrent inhibition. Thus they fire at low rates, even though they receive strong external excitatory inputs. The firing is irregular because the average total (external excitatory plus recurrent inhibitory) current is subthreshold, and firing is triggered by fluctuations due to noise in external and recurrent inputs. On the other hand, the oscillation is stable because of the repetitive succession of the following events: at the peak of a cycle, there is strong inhibitory firing. After a time lag of ~2.5 ms due to synaptic filtering, every neuron in the network feels a massive inhibitory input and activity goes down, hence the trough in global activity. Subsequently, ~2.5 ms later, the synaptic currents decay away, the total input becomes high due to strong external stimulation, and there is another surge of activity. The period of the oscillation is therefore about two times the synaptic lag, i.e., 5 ms in this case. Qualitatively, the oscillation is as described by Brunel and Hakim (1999). In the following text, we present an approximate analytical approach to quantitatively predict the population oscillation frequency.

Without recurrent inhibitory interactions, neurons would show asynchronous spike discharges due to external excitatory drive. This asynchronous state is destabilized, and synchronous

oscillation emerges, when inhibitory recurrent feedback becomes sufficiently strong. The inhibitory feedback can be enhanced in different ways: by increasing either the coupling strength (the number of connections per neurons, the synaptic conductance) or the average inhibitory firing rate through an increase in external excitatory currents. Figure 2 shows how synchrony depends on the magnitude of the external excitatory input. In the "thermodynamical" (large N) limit, synchrony appears above some critical level of external stimulation ($\sim$10 kHz). Firing rates of interneurons increase quasi-linearly with the external input as expected in strongly coupled networks (Brunel 2000; van Vreeswijk and Sompolinsky 1996). On the other hand, the frequency of the population oscillation stays relatively constant, between 150 and 200 Hz. Therefore the network frequency is independent of single cell firing rate and depends only weakly on the magnitude of external drive. This dissociation between network oscillation frequency and single neuron firing rate will be confirmed below by analytical calculations.

Analytical approach for predicting the network frequency

In this section, we outline our approach for one population of inhibitory neurons. Later, we will extend the method to two populations of excitatory and inhibitory cells. The instantaneous firing rate of the interneuronal population $\nu_I(t)$ is defined as the fraction of neurons firing in a short interval $[t, t + dt]$ where dt is small, divided by dt. In an asynchronous state, the firing rate is stationary (independent of time) apart from finite size effects. The population firing rate ν_I is determined by the sum of two synaptic currents, the excitatory external drive I_{ext} and the feedback inhibition I_{GABA}. I_{GABA} in turn depends on the population activity, hence is a function of ν_I itself. Given a presynaptic firing rate ν_{pre}, one can calculate the synaptic current $I_{GABA}(\nu_{pre})$. Then the postsynaptic firing rate as a function F of the sum $I_{syn}(\nu_{pre}) = I_{ext} - I_{GABA}(\nu_{pre})$ can be evaluated, $\nu_{post} = F[I_{syn}(\nu_{pre})]$. Finally, because both the pre- and postsynaptic firing rates are of the same neural population, they must be the same and equal to ν_I. Hence, $\nu_I = F[I_{syn}(\nu_I)]$ yields a self-consistent equation for ν_I.

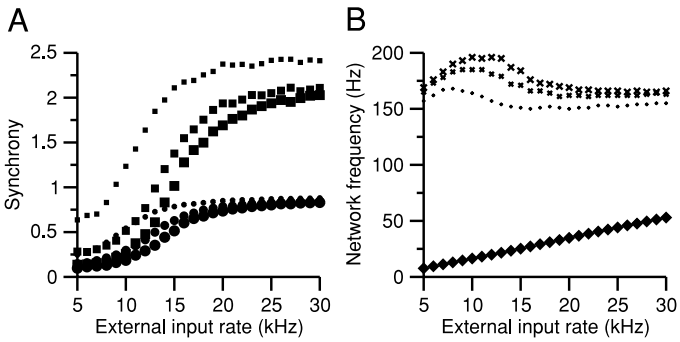

FIG. 2. Dependence of population oscillation on the external drive. *A*: network coherence measured by the spike synchrony index STS (square) and membrane synchrony index MPS (circle; see METHODS). Small symbols: 500 neurons, connection probability 0.4; medium symbols: 1,000 neurons, connection probability 0.2; large symbols: 2,000 neurons, connection probability 0.1. Other parameters as in Fig. 1. Below a critical external drive ($\sim$10 kHz), the synchrony indices decrease to zero with increased network size and the network is asynchronous. Above this critical external drive, the synchrony indices converge to a level that is independent of the network size. The network becomes oscillatory and coherent. *B*: the average firing rate of single cells increases linearly with the external drive (diamond), whereas the network oscillation frequency ($\times$ with 3 different population sizes) is relatively constant and independent of the external drive or single cell firing rate.

To understand whether asynchrony or synchrony is present in the network, a linear stability analysis of the asynchronous state is performed (Abbott and van Vreeswijk 1993; Brunel and Hakim 1999; Treves 1993). Small deviations around the stationary state, in which the instantaneous firing rate is a sum of a stationary firing rate ν_{I0} plus a small exponential component $\nu_{I0}\epsilon_I \exp(\mu t + i\omega t)$, where $\epsilon_I \ll 1$, are considered. When $\mu < 0$, this corresponds to a damped oscillation with frequency ω; when $\mu = 0$, this corresponds to a sinusoidal wave around the stationary state; when $\mu > 0$, this corresponds to an oscillation that amplifies with time. Thus self-consistent solutions of network activity with $\mu > 0$ signal an oscillatory instability: an oscillation with a finite amplitude develops from the asynchronous state. The onset of synchrony is therefore signaled by the appearance of solutions with $\mu = 0$. Here, we investigate the conditions under which the network activity has a sinusoidal component with $\mu = 0$. In such a way we obtain the population frequency close to the onset of oscillations.

Specifically, the procedure can be decomposed in the following four steps.

STEP 1. ASSUME A PRESYNAPTIC RHYTHMIC FIRING RATE. The instantaneous population firing rate is assumed to have the form

$$\nu_I(t) = \nu_{I0}[1 + \epsilon_I \exp(i\omega t)] \quad (1)$$

where ν_{I0} is the average firing rate, ϵ_I is the relative modulation of the oscillatory deviation to the stationary firing rate, and ω is the frequency of the network oscillation.

STEP 2. OBTAIN THE POST-SYNAPTIC CURRENT FROM THE PRESYNAPTIC FIRING RATE. We next calculate the synaptic conductance produced by presynaptic cells firing at the rate $\nu_I(t)$. The sum of all inhibitory synaptic variables in a given cell s_I is given by the sum of two exponentials (see METHODS) or equivalently by

$$\tau_r \frac{dx}{dt} = \tau_m \sum_{i,j} \delta(t - t_{i,j} - \tau_I) - x \quad (2)$$

$$\tau_d \frac{ds_I}{dt} = x - s_I \quad (3)$$

where $\sum_{i,j}\delta(t - t_{i,j})$ is the compound spike train of all presynaptic neurons connected to the cell. In average, a postsynaptic cell receives inputs from $C_I = pN_I$ presynaptic cells, where p is the connection probability and N_I is the total number of interneurons in the network. The variables s_I and x obey the equations

$$\tau_r \frac{dx}{dt} = \tau_m C_I \nu_I(t - \tau_I) + \text{fluctuations} \quad (4)$$

$$\tau_d \frac{ds_I}{dt} = x - s_I \quad (5)$$

in which the spike train has been replaced by the sum of the instantaneous firing rate $\nu(t - \tau_I)$ and random fluctuations. Solving these two equations, we obtain the average synaptic variable $s_I(t)$, which has the same form as the firing rate $\nu_I(t)$ but with an amplitude attenuation factor $S_I(\omega)$ and a phase shift $\Phi_I(\omega)$. More precisely

$$s_I = s_{I,0}[1 + \epsilon_I S_I(\omega) \exp(i\omega t - i\Phi_I(\omega))] + \text{fluctuations} \quad (6)$$

where $s_{I,0}$ is the average synaptic variable

$$S_I(\omega) = \frac{1}{\sqrt{(1 + \omega^2\tau_{dI}^2)(1 + \omega^2\tau_{rI}^2)}} \quad (7)$$

and

$$\Phi_I(\omega) = \omega\tau_{lI} + \text{atan}(\omega\tau_{rI}) + \text{atan}\,(\omega\tau_{dI}) \quad (8)$$

Note that the phase lag is the sum of three terms corresponding to the three distinct phases of the synaptic current: the lag due to latency is linear in ω; the lag due to the rise time; and the lag due to the decay time. The latter two lags are linear in ω at low frequencies and saturate at $\pi/2$ at high frequencies.

Neglecting temporal variations in the driving force, the GABAergic synaptic current is simply s_I multiplied by a constant factor

$$I_{GABA} = I_{GABA,0}[1 + \epsilon_I S_I \exp(i\omega t - i\Phi_I(\omega))] + \text{fluctuations} \quad (9)$$

where $I_{GABA,0}$ is the average GABAergic current. It is proportional to the maximum synaptic conductance g_{GABA} and the average number of synaptic contacts C_I, $I_{GABA,0} \sim g_{GABA}C_I$.

The GABAergic current experienced by the neuron is therefore the sum of three terms: an average drive $I_{GABA,0}$ due to the average firing rate ν_{I0} of inhibitory cells; an oscillatory component due to the global oscillation; and a noisy component due to the random arrival of spikes, after filtering by the synaptic kinetics. The total synaptic current is

$$\begin{aligned} I_{syn} &= I_{ext} - I_{GABA,0}[1 + \epsilon_I S_I(\omega) \exp(i\omega t - i\Phi_I(\mu, \omega))] + I_{noise} \\ &= I_{tot,0}\left[1 + \epsilon_I S_I \frac{I_{GABA,0}}{I_{tot,0}} \exp(i\omega t + i\pi - i\Phi_I(\omega))\right] + I_{noise} \end{aligned} \quad (10)$$

where $I_{tot,0}$ is the total average synaptic current, and I_{noise} is the random component. The factor π in the phase appears because of the minus sign introduced by inhibitory interactions.

STEP 3. OBTAIN THE POSTSYNAPTIC FIRING RATE FROM THE POSTSYNAPTIC CURRENT. We now calculate the postsynaptic firing rate $\nu_I(t)$ in response to the synaptic current I_{syn} (*Eq. 10*). For a synaptic input $I_{syn}(t)$ that varies periodically in time, the response $\nu_I(t)$ is expected in general to depend on the frequency ω of the oscillatory input. For example, one might expect both amplitude change and phase shift between the oscillatory components of I_{syn} and ν_I at high frequencies ω. Therefore, in general, the input-output relationship between $I_{syn}(t)$ and $\nu_I(t)$ is expected to depend explicitly on ω. This subject has been analytically investigated in (Brunel et al. 2001; Fourcaud and Brunel 2002) for the LIF neuron model. It was found that when synaptic time constants are very fast compared to the membrane time constant, $\nu_I(t)$ shows a phase lag with respect to $I_{syn}(t)$ and the amplitude of the modulation is attenuated at high frequencies. On the other hand, with a sufficient amount of noise filtered by synaptic time constants that are of the order of the membrane time constant, the postsynaptic firing rate follows instantaneously the variations in input currents. In other words, the response of the neuron to oscillatory currents at frequency ω has an amplitude that is nearly *independent* of the frequency and has *no phase lag*. The specific conditions for this to be true are: single neurons are described by the LIF model; synaptic noise is of large amplitude and with a decay times are comparable to the membrane time constant; and the variations in input currents are such that the firing rate remains strictly positive.

Under these conditions, the dynamics of our network can be described by firing rate dynamics that are purely determined by the synaptic time constants. Specifically, the firing rate is simply a function of the total synaptic current

$$\nu_I(t) = F(I_{syn}(t)) \quad (11)$$

where F is the current-frequency function. Because the oscillation amplitude ϵ_I is small, we can expand this function as $F(I_{syn}(t)) \simeq F(I_{tot,0}) + F'(I_{tot,0})(I_{syn}(t) - I_{tot,0})$, where F' is the derivative of F with respect to the input current. Combining *Eq. 10* with *Eq. 11*, the firing rate of a cell is approximately given by

$$\nu_I(t) = \nu_{I,0}\left[1 + \epsilon_I S_I(\omega) \frac{I_{GABA0}}{I_{tot,0}} A_I \exp(i\omega t + i\pi - i\Phi_I(\omega))\right] \quad (12)$$

where $\nu_{I,0} = F(I_{tot,0})$ and $A_I = F'(I_{tot,0})I_{tot,0}/\nu_{I,0}$ is the relative variation in firing rate due to a relative variation in input current. A_I is proportional to the slope of the *f-I* curve F, normalized in such a way as to be dimensionless. For example, if the firing rate increases by 10% when the input current is increased by 10%, then $A_I = 1$.

STEP 4. SELF-CONSISTENT EQUATION FOR THE FIRING RATE. The last step is to equate the postsynaptic firing rate (*Eq. 12*) with the presynaptic firing rate (*Eq. 1*), yielding a self-consistent equation for the firing rate of neurons in the network

$$1 = S_I(\omega) \frac{I_{GABA0}}{I_{tot,0}} A_I \exp(i\pi - i\Phi_I(\omega)) \quad (13)$$

For the left- and right-hand sides to be equal, two relations have to be satisfied, one for the amplitude

$$1 = S_I(\omega) \frac{I_{GABA0}}{I_{tot,0}} A_I \quad (14)$$

and one for the phase

$$\pi = \Phi_I(\omega) = \omega\tau_{lI} + \text{atan}\,(\omega\tau_{rI}) + \text{atan}\,(\omega\tau_{dI}) \quad (15)$$

The phase condition, *Eq. 15*, allows to determine the frequency of the network oscillation ω in terms of the synaptic temporal parameters. Using the frequency given by *Eq. 15*, *Eq. 14* can be solved to determine the value of a particular network parameter for which the onset of the oscillation occurs. For example, an increase in the synaptic connection strength increases the ratio $I_{GABA0}/I_{tot,0}$. The value of the synaptic connection strength beyond which synchronized oscillations occur can therefore be obtained from *Eq. 14* once S_I and A_I are known.

How network frequency depends on the synaptic time constants

The phase *Eq. 15* indicates that the frequency ω of the population oscillation at the onset of oscillations is purely determined by the synaptic parameters τ_{lI}, τ_{rI}, and τ_{dI}. This is illustrated graphically in Fig. 3*B*, for the same model parameters as the network simulation of Fig. 1. The function $\Phi_I(\omega = 2\pi f)$ is plotted against the frequency f, the intersection of this curve with the horizontal line $\Phi = \pi$ occurs at the population

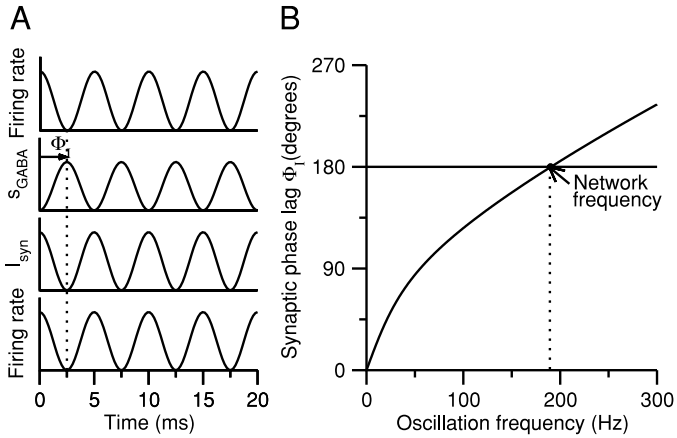

FIG. 3. Theoretical prediction of the network oscillation frequency. *A*: When the firing rate has an oscillatory component, the fraction of open channels at inhibitory synapses is also oscillatory but with a phase shift $\Phi_I(\omega)$ due to the temporal characteristics of the synaptic processing. The total synaptic current $I_{syn} = I_{ext} - I_{GABA}$ is phase-reversed compared to $s(t)$. Due to the characteristics of noise, the firing rate is proportional to I_{syn} with no phase shift. *B*: Φ_I is plotted against the frequency $f = \omega/2\pi$ (black). The intersection with the horizontal line at 180 degrees gives the network frequency $f_{pop} \simeq 180$ Hz. See text for discussion. Same parameters as in Fig. 1.

frequency f_{pop}, according to *Eq. 15*. For the parameters of Fig. 1, the theoretically predicted frequency of $f_{pop} \simeq 180$ Hz is very close to that of the simulated network oscillation (Fig. 1).

The dependency of the network frequency on the synaptic parameters is shown in Fig. 4. It is apparent that the network frequency is more sensitive to relative variations of the shortest time scales (the latency and the rise time) than to variations in the longest time scale (the decay time). To understand these observations theoretically, let us re-write *Eq. 15* with $\omega = 2\pi f$

$$\frac{1}{2} = f\tau_{ll} + \frac{1}{2\pi}\,\mathrm{atan}\,(2\pi f\tau_{rI}) + \frac{1}{2\pi}\,\mathrm{atan}\,(2\pi f\tau_{dI}) \qquad (16)$$

Because the atan function is bounded from above by $\pi/2$, the right-hand side of *Eq. 16* can be equal to ½ only with a strictly positive latency τ_{ll}. Therefore the latency of synaptic transmission is critical for the emergence of coherent oscillations in this model. Furthermore, simple bounds for the population frequency can be obtained using the inequalities $\mathrm{atan}(x) < x$, $\mathrm{atan}\,(x) < \pi/2$ and $\mathrm{atan}\,(x) > \pi/2 - 1/x$

$$\frac{1}{4(\tau_{ll} + \tau_{rI})} < f_{pop} < \frac{1}{2\pi}\sqrt{\frac{1}{\tau_{ll}\tau_{rI}} + \frac{1}{\tau_{ll}\tau_{dI}}}$$

Thus the period of the oscillation must be shorter than four times the sum of the latency and the rise time. The upper bound of the frequency has a more complicated form, but can be simplified when τ_{rI} is much shorter than the decay time τ_{dI}. Indeed, voltage-clamp measurements of $GABA_A$ receptor-mediated IPSCs show that the latency and rise time are of the order of $\leq$1 ms, while the decay time is longer, of order 5–10 ms (Bartos et al. 2001, 2002; Gupta et al. 2000; Kraushaar and Jonas 2000; Salin and Prince 1996; Xiang et al. 1998). When the decay time is much slower than the rise time, $\tau_{dI} \gg \tau_{rI}$, the bound becomes

$$\frac{1}{4(\tau_{ll} + \tau_{rI})} < f_{pop} < \frac{1}{2\pi\sqrt{\tau_{ll}\tau_{rI}}}$$

Thus the period of the oscillation must be longer than about six times the geometrical mean of latency and rise times. These bounds indicate that the frequency is mostly controlled by the shorter time scales (τ_{ll} and τ_{rI}) because the bounds are independent of τ_{dI}. They provide a simple way to estimate the order of magnitude of the network frequency. For example, if $\tau_{ll} = \tau_{rI} = 1$ ms, we obtain 125 Hz $< f_{pop} <$ 159 Hz. For the parameters of Fig. 1 ($\tau_{ll} = 1$ ms, $\tau_{rI} = 0.5$ ms), 167 Hz $< f_{pop} <$ 225 Hz in agreement of the observed frequency of 180 Hz.

Figure 4 shows how the degree of network synchronization, or the oscillation amplitude, depends on the three synaptic time constants. The simulation results can be qualitatively understood with the help of our theoretical analysis. The synaptic time constants affect the degree of synchrony in two ways: through the dependency of $S_I(\omega)$, as described by *Eq. 7*, and through a change of oscillation frequency, as governed by *Eq. 15*. The attenuation factor S_I does not depend on the latency τ_{ll} explicitly. An increase in τ_{ll} affects the degree of synchrony only indirectly through a decrease in the population frequency. The attenuation due to synaptic filtering is smaller at lower frequencies, hence the network oscillation is amplified with a

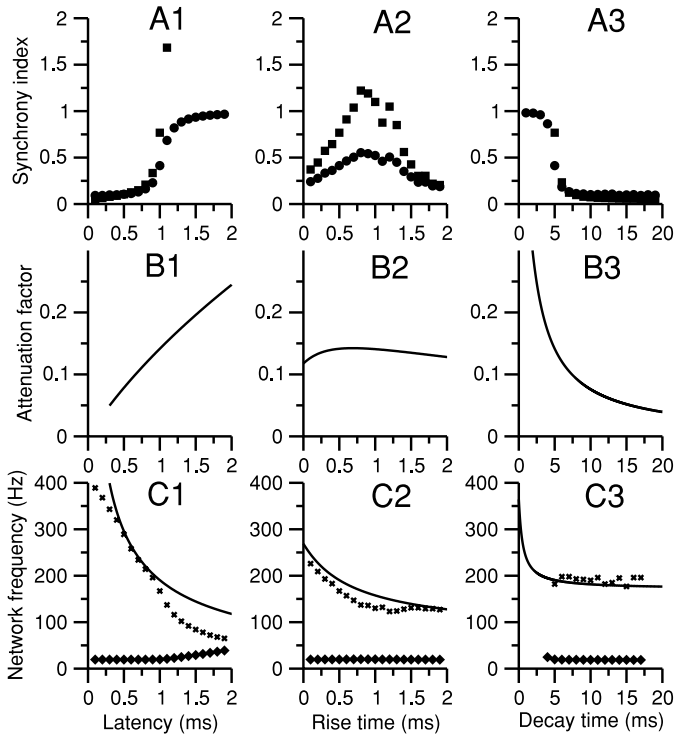

FIG. 4. Frequency of population oscillation as a function of synaptic temporal parameters. The control parameter set is $\tau_{ll} = 1$ ms, $\tau_{rI} = 0.5$ ms, $\tau_{dI} = 5$ ms. *A*: synchrony indices as synaptic parameters are varied (*A*1: latency, *A*2: rise time, *A*3: decay time). ●, membrane synchrony index. ■, spike synchrony index. *B*: synaptic attenuation factor at the network frequency predicted by the theory, given by $S_I(\omega = 2\pi f_{pop})$ (*B*1: latency, *B*2: rise time, *B*3: decay time). This factor gives the amplitude of the modulation of the synaptic currents by a sinusoidal presynaptic input at frequency ω, divided by the amplitude of a modulation at 0 frequency. The smaller this factor, the more asynchronous the network. Here, transition to synchrony occurs when this factor is ~0.15. *C*: network frequency vs latency (*C*1), rise time (*C*2), and decay time (*C*3). Note that the network frequency decreases dramatically with the latency (*A*) and rise time (*B*), but not significantly with the decay time (*C*). Full line: solution of *Eq. 15*. ×: network frequency in the simulations. ◆, single cell frequency in the simulations. Parameters as in Fig. 1.

longer latency τ_{lI}. Changes in the rise time τ_{rI} have two effects: an increase of τ_{rI} decreases S_I through the $1/\sqrt{1+\omega^2\tau_{rI}^2}$ factor in *Eq. 7;* but it also reduces the population frequency ω, for the same reason as for the latency. These two opposing effects tend to counterbalance each other. As long as the rise time is of the same order as the latency and shorter than the decay time, the decreased ω dominates over the increased τ_{rI}, so that the product $\omega\tau_{rI}$ is smaller, and the network synchrony is higher with a larger τ_{rI}. For longer rise times, the attenuation factor has a stronger influence and becomes predominant, thus the oscillation amplitude decreases. Finally, a longer decay time decreases the amplitude of the oscillation. This is because the decay time has little effect on the frequency, but on the other hand, it increases the attenuation by synaptic filtering due to the factor $1/\sqrt{1+\omega^2\tau_{dI}^2}$ in *Eq. 7.*

In summary, recurrent synaptic inhibition with a large latency and very short rise and decay times, i.e., close to a delayed delta function, lead to pronounced oscillations. On the contrary, IPSCs with negligible latency lead to asynchrony in a network of leaky integrate-and-fire neurons. This feature is crucially dependent on the fact that the neuronal firing rate follows instantaneously (i.e., without phase lag) inputs at any frequency. If a neuronal phase lag is present, as expected for Hodgkin-Huxley conductance-based neurons, then network synchrony can be obtained even in absence of a latency. However, in general we expect that large synaptic latency tends to facilitate synchrony.

Above the onset of oscillations, the oscillation amplitude becomes large, and our theoretical analysis is no longer valid. Numerical simulations show that the network frequency decreases and network coherence increases, similar to what happens in the simplified network of Brunel and Hakim (1999). For very high external inputs, the firing rate of single neurons becomes comparable to the network frequency. The network reaches an almost fully synchronized state with regularly firing neurons and therefore enters the regime of coupled oscillators.

Two population networks

OSCILLATIONS DUE TO PYRAMIDAL-INTERNEURON FEEDBACK LOOP. An alternative to the interneuronal network model of fast oscillations is the feedback inhibition model: pyramidal neurons excite interneurons, which in turn send inhibition back onto pyramidal cells (Freeman 1975; Jefferys et al. 1996; Leung 1982). In a recent slice experiment (Fisahn et al. 1998), spontaneously occuring 40-Hz oscillations have been shown to depend both on the excitatory and inhibitory synaptic transmissions. Both types of loops (pyr → int → pyr and int → int) are present in a cortical network. The two preceding mentioned mechanisms are not necessarily mutually exclusive and may cooperate in the generation of a coherent network rhythm.

To understand how the pyramidal-interneuron loop is involved in the generation of population synchrony, it is useful to consider first the feedback inhibition scenario in isolation, in which only pyramidal-to-interneuron and interneuron-to-pyramidal connections are present (no pyramidal-to-pyramidal and no interneuron-to-interneuron connections).

In this scenario, it is straightforward to repeat the analysis of the previous section (see APPENDIX 1 for details). The population frequency is now given by

$$\pi = \Phi_I(\omega) + \Phi_E(\omega) \tag{17}$$

$$= \omega\tau_{lI} + \text{atan}\,(\omega\tau_{rI}) + \text{atan}\,(\omega\tau_{dI}) + \omega\tau_{lE} + \text{atan}\,(\omega\tau_{rE}) + \text{atan}\,(\omega\tau_{dE}) \tag{18}$$

Thus the population frequency is now determined by the sum of excitatory and inhibitory synaptic phase lags. This leads to a decrease of the population frequency compared to the purely interneuronal scenario due to the additional excitatory synaptic phase lag. Furthermore, in this scenario, the inhibitory neurons lag behind the excitatory neurons by $\Phi_E(\omega)$ (see *Eq. A9* in APPENDIX 1). In particular, if synaptic time scales of excitation and inhibition are identical, then $\Phi_E(\omega) = \Phi_I(\omega) = \pi/2$, hence interneurons lag pyramidal cells by 90°, and the population frequency will be more than halved compared to the frequency of the purely interneuronal network.

As an example, we take GABA synapses with latency τ_{lI} = 0.5 ms, rise time τ_{rI} = 0.5 ms, decay time τ_{dI} = 5 ms, and AMPA synapses with latency τ_{lI} = 1 ms, rise time τ_{rI} = 0.4 ms, and decay time τ_{dI} = 2 ms. In the purely interneuronal scenario, f_{pop} is equal to 296 Hz, while in the E-I loop scenario, the frequency goes down to 79 Hz, with interneurons lagging behind pyramidal cells by 104°—a drastic reduction in population frequency.

In the presence of both types of feedback loops (E-I loop and I-I loop), a network tends to settle in an oscillation that is a compromise between the two scenarios with a frequency and phase lag that are intermediate between these two extremes. The frequency and phase lag are then determined by the relative strength of the E-I and I-I connections through *Eqs. B9* and *B10* of APPENDIX 2. As an example, Fig. 5 shows a simulation of a two-population network without pyramid-to-pyramid connections. Note that such a network could represent a simplified model for a CA1 network where pyramid to pyramid connections are rare. The synaptic conductances are as indicated in METHODS. With a small external drive, the network is essentially asynchronous, and the power spectrum of the population firing rate is flat (Fig. 5*A*). When the external drive is sufficiently strong, coherent 200-Hz oscillations emerge in the network. In this oscillation, the interneurons lag behind pyramidal cells by ~90°. Note that for the synaptic parameters chosen here, a one-population interneuronal network would oscillate at ~300 Hz (see Fig. 4*C*1). Thus the pyramidal-interneuron loop slows down the oscillation significantly from 300 to 200 Hz. Both pyramidal cells and interneurons fire intermittently at much lower rates than the population rhythm, and there is a broad distribution of firing rates across individual cells (3–150 Hz, average: 50 Hz) for interneurons, 1–20 Hz, average: 7 Hz) for pyramidal cells. Neurons in CA1 show similar intermittent spike activity during sharp wave ripples in vivo (Buzsaki et al. 1992; Csicsvari et al. 1998, 1999b).

Effect of pyramidal-to-pyramidal connections on oscillations

To understand the effect of pyramidal-to-pyramidal connections on oscillations, it is useful to consider first a network in which only these connections are present. In such networks, it is straightforward to show that instabilities can only occur with $f = 0$ Hz (a rate instability). Adding pyramidal-to-pyramidal connections to a network with all other types of connections tends again to decrease network frequency because these connections tend to prolong the positive phases of each cycle of the oscillation. The observed frequency and phase lags between the two populations is now a compromise between the

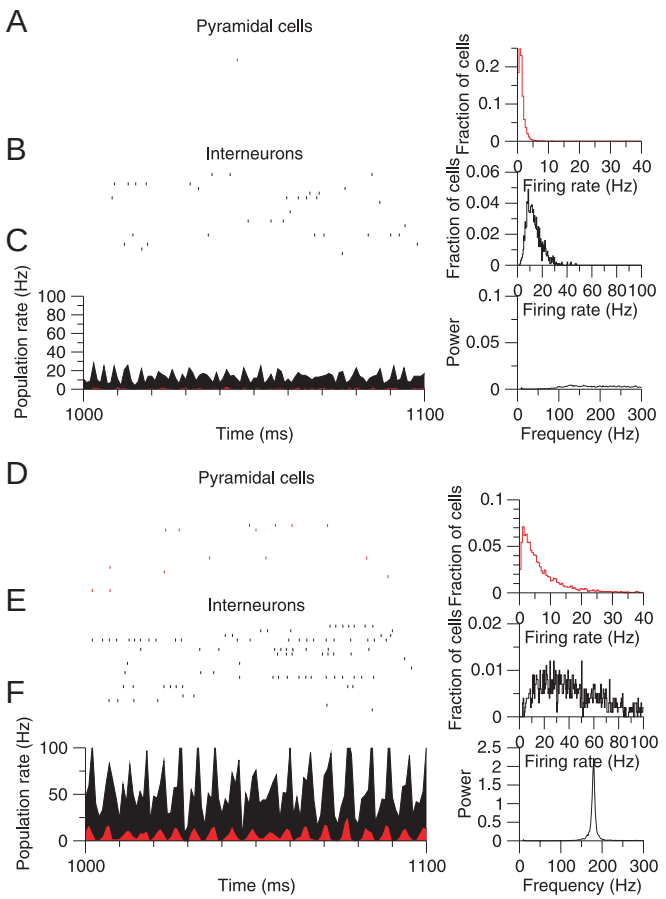

FIG. 5. Two-hundred-Hz oscillations in a network with pyramidal cells and interneurons, but without pyramid-to-pyramid connections. *A–C*: low external input (6 kHz for both populations). *A*: pyramidal population rastergram (*left*) and distribution of firing rates across pyramidal cells (*right*). *B*: interneuron population rastergram (*left*) and distribution of firing rates across interneurons (*right*). *C*: instantaneous population firing rate (black: interneuron, red: pyramid) (*left*) and its power spectrum (*right*). The neural spike discharges are very sparse and asynchronous, the power spectrum of the population firing rate is virtually flat. *D–F*: high external input (24 kHz for pyramidal cells and 22 kHz for interneurons). Same conventions as *A–C*. There is a prominent synchronous oscillation of the population activity (*F*, *left*) and a sharp peak in the power spectrum (*F*, *right*). At the same time, single neurons, that collectively produces this population oscillation, show stochastic and intermittent spike trains, with a wide distribution of firing rates (*D* and *E*). The simulated network has 4,000 pyramidal cells and 1,000 interneurons; the connection probability is 0.2. Time constants for the GABA synapses: latency $\tau_{lI} = 0.5$ ms, rise time $\tau_{rI} = 0.5$ ms, decay time $\tau_{dI} = 5$ ms. Time constants for the AMPA synapses: latency $\tau_{lI} = 1$ ms, rise time $\tau_{rI} = 0.4$ ms, decay time $\tau_{dI} = 2$ ms.

strength of the all the feedback loops (E-E, E-I, and I-I), see *Eq. C3* of APPENDIX 3.

An example is shown in Fig. 6 of a network oscillation when the pyramid-to-pyramid excitatory connections are included into the model. The network architecture is now closer to that of the CA3 hippocampus, with extensive recurrent collaterals between pyramidal cells. The oscillation frequency is dramatically reduced by the insertion of such connections, from 200 to ~110 Hz (Fig. 6).

The two-population network, with all four (E-to-E, E-to-I, I-to-E and I-to-I) types of connections, displays fast oscillations which are typically in the frequency range of 30–110 Hz, depending on the synaptic time constants and on the balance between the loops. In Fig. 7 is shown a simulation with slightly

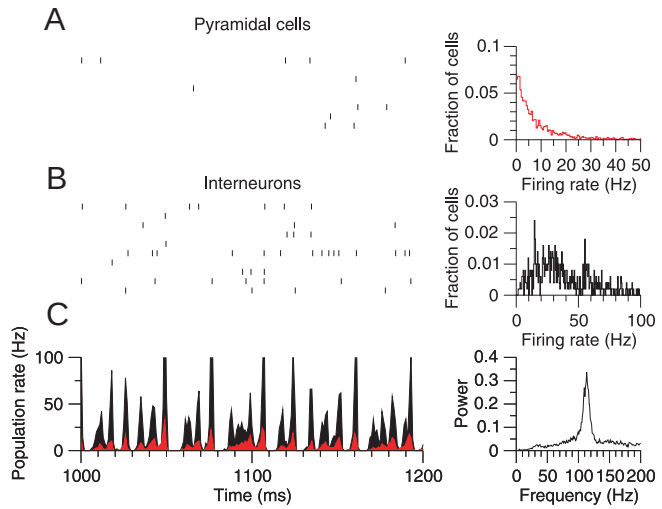

FIG. 6. Recurrent excitation between pyramidal cells decreases the population frequency. The inclusion of collateral connections between pyramidal cells reduces the population frequency from 200 to 110 Hz. Conventions as in Fig. 5. Pyramidal cells (*A*) and interneurons (*B*) show intermittent and irregular firing, while generating a coherent network rhythm as evident in the population firing rate and its power spectrum (*C*). External input rate is 4 kHz. Time constants: for the I → E and I → I synapses, latency $\tau_{lI} = 0.5$, ms, rise time $\tau_{rI} = 0.5$ ms, decay time $\tau_{dI} = 5$ ms. For the E → E synapses: latency $\tau_{lE} = 0.5$ ms, rise time $\tau_{rE} = 0.4$ ms, decay time $\tau_{dE} = 2$ ms. For the E → I synapses: latency $\tau_{lE} = 0.5$ ms, rise time $\tau_{rE} = 0.2$ ms, decay time $\tau_{dE} = 1$ ms.

longer (latency and decay) time constants of synaptic inhibition, compared to Fig. 6. With slower inhibition, the network oscillation frequency is lower (50 instead of 110 Hz). In this case, the model reproduces the salient characteristics of 40-Hz oscillations in CA3 (Fisahn et al. 1998) and neocortical (Buhl et al. 1998) slices. During 40-Hz population rhythm, single-cell firing rates are low, ~10 Hz in interneurons and 2 Hz in pyramidal cells, in average. Spike trains of individual neurons

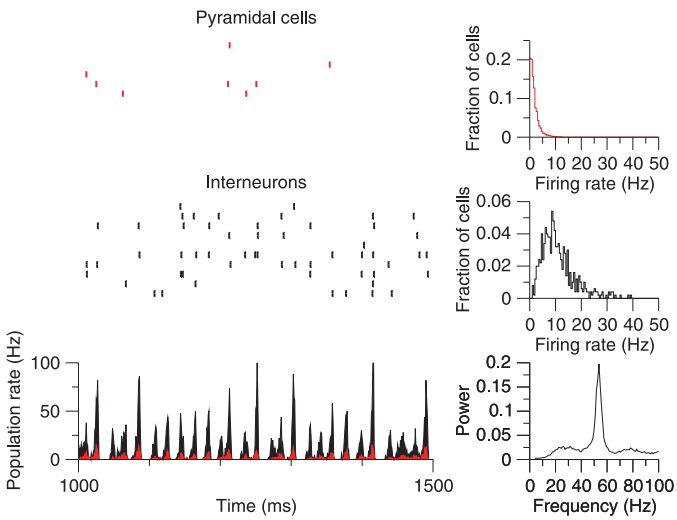

FIG. 7. Gamma oscillations in a two-population network. Same parameters as in Fig. 6 except that some synaptic time constants are slightly longer. Conventions as in Fig. 5. Pyramidal cells (*A*) and interneurons (*B*) show intermittent and irregular firing, while generating a coherent rhythm at 40 Hz in the population firing rate (*C*). External input rate is 2.6 kHz. Time constants: for the I-to-E and I-to-I synapses, latency $\tau_{lI} = 1.5$ ms, rise time $\tau_{rI} = 1.5$ ms, decay time $\tau_{dI} = 8$ ms. For the E-to-E synapses: latency $\tau_{lE} = 1.5$ ms, rise time $\tau_{rE} = 0.4$ ms, decay time $\tau_{dE} = 2$ ms. For the E-to-I synapses: latency $\tau_{lE} = 1.5$ ms, rise time $\tau_{rE} = 0.2$ ms, decay time $\tau_{dE} = 1$ ms.

are irregular and intermittent. It would be difficult to detect the oscillation from such analysis as autocorrelation function and power spectrum of spike trains. However, a subthreshold oscillation is apparent in the membrane potential traces. The membrane potential hovers below and near the firing threshold. Spikes are triggered randomly by noise fluctuations, leading to sparse and irregular spike trains. As in the experiments, network oscillation was abolished in the model by blockade of either AMPA-mediated excitation or GABA-mediated inhibition but not NMDA-mediated excitation. Thus the salient observations of these experiments (Fisahn et al. 1998; Buhl et al. 1998) can be reproduced and understood in this simple setting.

Phase shift between two populations

Recurrent excitation also tends to decrease the phase shift between excitatory and inhibitory populations. In the absence of pyramidal-to-pyramidal connections, interneurons can lag excitatory cells by >90° as shown in the preceding text. When pyramidal-to-pyramidal connections are present and the balance between inhibition and excitation is equal in pyramidal cells and interneurons, the analysis predicts that the phase shift becomes essentially zero (see APPENDIX 3 for details). Figure 8 shows that the zero phase shift is indeed observed in simulations where these conditions hold. In hippocampal slices, where gamma oscillation appears to depend on the pyramid-interneuron connections, Fisahn et al. (1998) found no significant phase shift between spike activities of pyramidal and interneuronal populations. Significant phase lag was seen only between pyramidal cell firing and EPSCs and IPSCs. This observation is reproduced by our model, where pyramidal and interneuronal spiking activities are synchronized with zero phase difference. EPSCs and IPSCs lag behind the pyramidal spiking by 2 and 5 ms, respectively (Fig. 8). These phase lags can be simply accounted for by the time-to-peak of the excitatory and inhibitory synaptic currents. Therefore gamma oscillation in a pyramid-interneuron network is compatible with zero phase difference between pyramidal cells and interneurons like in the experiment of Fisahn et al. (1998). The simple intuitive reason for this phenomenon is that if the balance of excitation and inhibition is the same in pyramidal cells and interneurons, the inputs to both cell types must be in phase, and hence the firing rates of both cell types must also be in phase.

Dependence of oscillation frequency on the balance and relative speeds of excitation and inhibition

To understand better the two-population network with all four (E-to-E, E-to-I, I-to-E, and I-to-I) connections, we analyzed the oscillatory behavior under the assumption that the ratio of AMPA to GABA conductances is equal in pyramidal cells and interneurons, as a reasonable working hypothesis for neocortical and CA3 networks. Hence the ratio I_{AMPA}/I_{GABA} is the same for both pyramidal cells and interneurons.

In such a network, the analysis predicts that the frequency strongly depends on the balance between AMPA and GABA synaptic currents (*Eq. C6* of APPENDIX 3). This is a manifestation of the fact that both pyramidal-to-interneuron connections (via the E-I loop) and the pyramidal-to-pyramidal connections tend to decrease population frequency. In the simulations shown in Fig. 9, we varied systematically the balance between

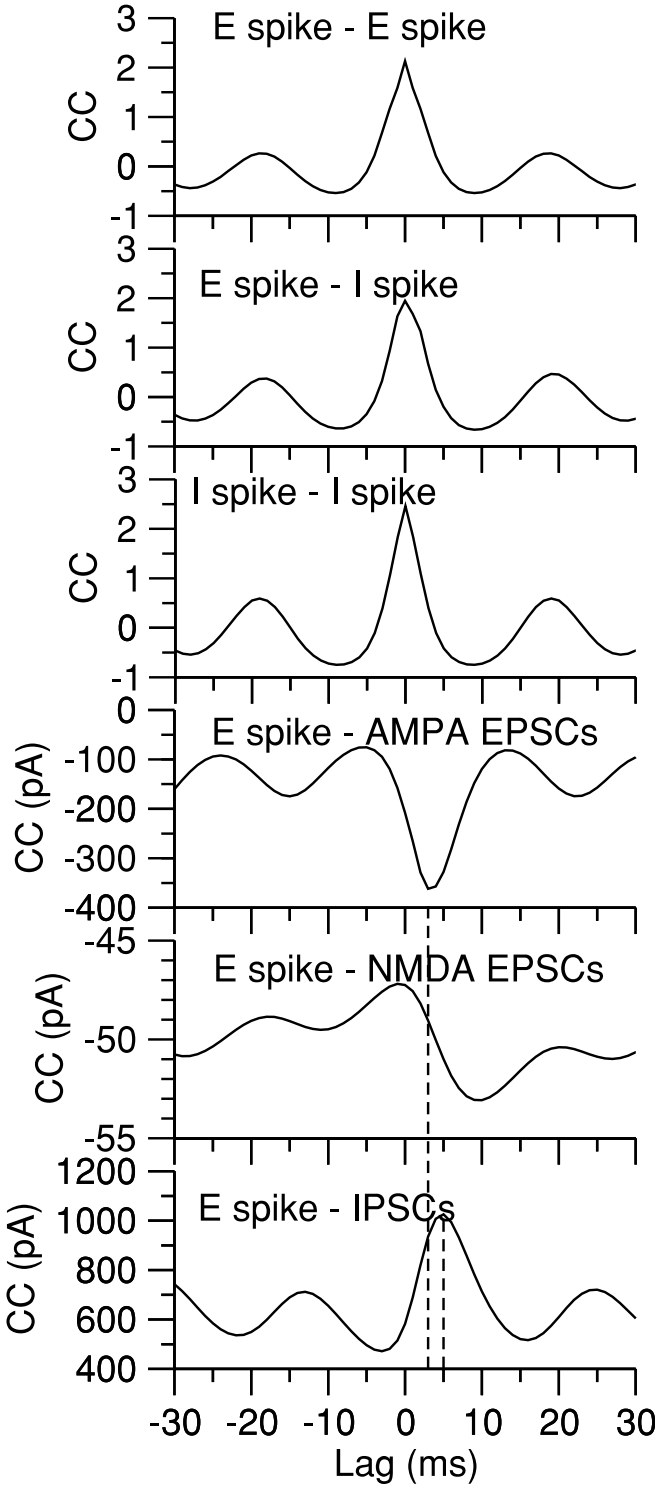

FIG. 8. Temporal correlations during gamma oscillation. There is 0 phase shift between pyramidal cells and interneurons in the population spiking cross-correlation. With respect to spiking activity, there is a phase lag of 2, 10, and 5 ms, for AMPA-, NMDA-, and GABA-mediated synaptic currents, respectively. These phase delays are due to the time-to-peak of the synaptic currents. The cross-correlation functions between pyramidal firing and excitatory and inhibitory postsynaptic currents (EPSCs and IPSCs) are similar to the experimental observations (Fisahn et al. 1998) with comparable phase lags. Our model predicts that the 0 phase difference between spiking activities of pyramidal and interneuronal populations is a manifestation of the same excitation-inhibition balance in pyramidal cells and interneurons. See text for further discussion.

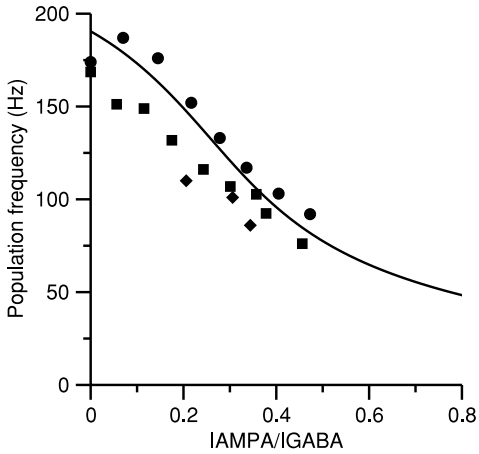

FIG. 9. Population oscillation frequency decreases with the recurrent excitation/inhibition balance. The ratio I_{AMPA}/I_{GABA} is the same for both pyramidal cells and interneurons. The ratio is changed by varying the AMPA conductance on both pyramidal cells and interneurons from 0 to 100% of the "control" value indicated in METHODS. The population frequency decreases from ~180 to 40 Hz. ——, analytical prediction (obtained by solving *Eq. C6*); symbols: network simulation data (●, 12-kHz external inputs; ◆, 6-kHz external inputs; ■, 4-kHz external inputs). Simulations with a too high synchrony (STS larger than 2.5) were discarded. The network has 4,000 pyramidal cells and 1,000 interneurons, with the connection probability of 0.2. Time constants for the GABA synapses: latency $\tau_{lI} = 1$ ms, rise time $\tau_{rI} = 0.5$ ms, decay time $\tau_{dI} = 5$ ms. Time constants for the AMPA synapses on both pyramidal cells and interneurons: latency $\tau_{lI} = 1$ ms, rise time $\tau_{rI} = 0.2$ ms, decay time $\tau_{dI} = 2$ ms.

I_{GABA} and I_{AMPA} by varying the AMPA conductances on both pyramidal cells and interneurons were varied from 0 to 100% of their "control" value (indicated in METHODS). When I_{AMPA}/I_{GABA} is increased from zero (without recurrent excitation, purely I-I oscillation) to 0.5 (strong recurrent excitation), the population frequency decreases from ~180 to 70 Hz (Fig. 9). The theoretical prediction (*Eq. C6*, ——) fits well with direct network simulations (●, ◆, ■). For these parameters, the ratio could not be increased beyond 0.5 in the simulation, because the network became very strongly synchronized, and hence the synchrony regime fell outside of the scope of the present study.

Unlike the one-population model where the network oscillation frequency depends only weakly on the synaptic decay time constant, the behavior of the two-population network also critically depends on the relative time constants of synaptic excitation and inhibition. As shown in Fig. 10, the parameter plane of the decay times τ_{AMPA} and τ_{GABA} is separated into two regions for the asynchronous and synchronous dynamics. The boundary between the two regions is the locus of the onset of synchronized oscillation (a bifurcation in the language of dynamical systems). Figure 10 shows that different values of the synaptic temporal parameters can favor one of the two competing kinds of oscillatory instabilities, the purely interneuronal mechanism or the pyramidal-interneuronal loop mechanism. This can be seen clearly along a horizontal line in Fig. 10*A* (say at fixed $\tau_{GABA} = 5$ ms). The asynchronous behavior is realized only in an intermediate range of τ_{AMPA} values. With very short τ_{AMPA}, oscillation occurs, as expected when excitation is faster than feedback inhibition (Tegnér et al. 2002; Tsodyks et al. 1997; Wang 1999; Wilson and Cowan 1973). With these short excitatory time constants, the E-I loop strongly influences the network oscillation, the population frequency is relatively low. On the other hand, with sufficiently long τ_{AMPA}, the excitatory synaptic current strongly attenuates the network oscillation. Driven by tonic excitation, the interneuronal network alone is able to generate a synchronous oscillation, which now has the characteristics of oscillation in the one-population model (with a very high population frequency). The population frequency is much higher when the oscillation is dominated by the interneuronal network (with

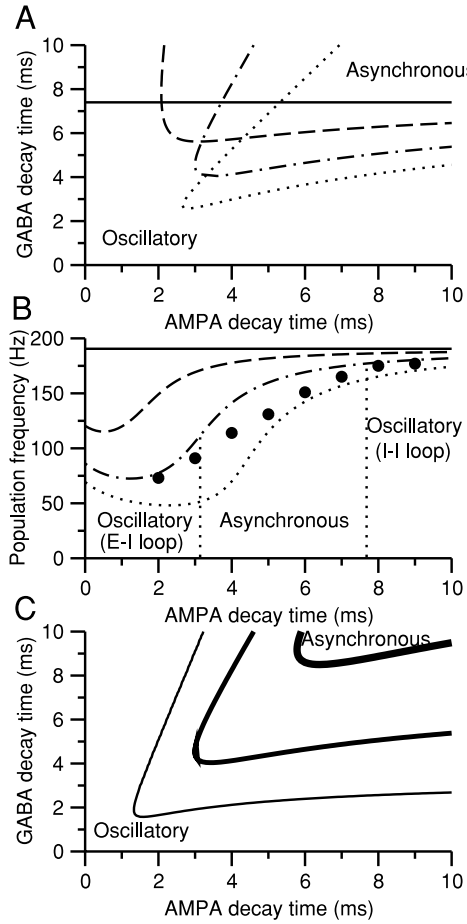

FIG. 10. Dependence of coherent fast oscillations on the relative time constants and balance of synaptic excitation and inhibition. *A*: network dynamical behavior on the parameter plane of τ_{AMPA} and τ_{GABA}. The asynchronous state is separated from the synchronous oscillation state by a "bifurcation" curve, obtained by *Eq. C5* of APPENDIX 3. The asynchronous state is stable on the top right corner of the figure. The strength of the I-I loop is set to $X_{II} = 10$ (see APPENDIX 3), and the balance between the AMPA and GABA currents is $I_{AMPA}/I_{GABA} = 0$ (full), 0.2 (- - -), 0.5 (- · -), 0.8 (· · ·). Qualitatively, there are 2 kinds of instability from asynchronous state to coherent oscillation. For a fixed τ_{GABA} (say at 5 ms), the asynchronous dynamics is destabilized and oscillation develops, when τ_{AMPA} becomes much smaller than τ_{GABA}, as a result of delayed negative feedback in a strongly recurrent network. On the other hand, when τ_{AMPA} is sufficiently large, the excitatory drive is roughly tonic and the interneuronal network by itself generates synchronous oscillation, similar to the 1-population model. *B*: population frequency as function of the excitatory synaptic decay time constant τ_{AMPA} with fixed $\tau_{GABA} = 5$ ms. The oscillation frequency is much lower with shorter τ_{AMPA} (the pyramid-interneuron loop regime) than with longer τ_{AMPA} (the interneuronal network regime). ——, theoretical predictions. ●, direct network simulations. Parameters as in Fig. 9 and METHODS. *C*: network state diagram for different strengths of recurrent connections again obtained from *Eq. C5*. Both g_{AMPA} and g_{GABA} are varied while preserving the balance $I_{AMPA}/I_{GABA} = 0.5$, $X_{II} = 20$ (top curve), 10 (middle curve), 5 (bottom curve). Coherent oscillations become more prevalent with stronger recurrence of the network. Synaptic parameters as in Fig. 9.

long τ_{AMPA}) than when it largely depends on the pyramid-to-interneuron loop (with short τ_{AMPA}; Fig. 10*B*).

The locus of the onset of synchrony is also greatly influenced by the strength and balance of excitation and inhibition, according to *Eq. C5* of APPENDIX 3. For the parameters of Fig. 10, without excitation (the ratio $I_{AMPA}/I_{GABA} = 0$), synchrony appears at $\tau_{GABA} = 7.5$ ms, independent of τ_{AMPA}. An increasingly large excitation/inhibition ratio shifts the bifurcation curve close to the diagonal line, and enlarges the oscillatory regime (at small τ_{AMPA}) dominated by the pyramid-interneuron loop (Fig. 10*A*). The population frequency is lower with a larger excitation/inhibition ratio (Fig. 10*B*), consistent with Fig. 9. Finally, with a fixed I_{AMPA}/I_{GABA} but enhancing the absolute connection strength (both g_{AMPA} and g_{GABA} are increased while their ratio is preserved), the parameter region for the asynchronous dynamics shrinks dramatically, and coherent oscillation becomes prevalent (Fig. 10*C*). Therefore powerful feedback synaptic interactions generally are destabilizing and favor large-amplitude coherent oscillations.

DISCUSSION

Summary of results

In this paper, we have extended a theoretical framework for understanding the mechanisms of fast network oscillations that are characterized by noisy and intermittent spike firing of constituent single cells. Brunel and Hakim (1999), using simple (instantaneous) synaptic interactions, showed that when the network is dominated by noise, coherent oscillation with irregular and sparse neuronal firing can be produced with strong recurrent inhibition and strong external excitation. In this paper, we extended this approach to a network of LIF neurons coupled by realistic synapses. Our analysis predicts the population frequency for noise-dominated network rhythms, given synaptic temporal parameters, and the balance between the different types of (I-I, E-I, E-E) feedback loops present in the network. This analysis based on a phase condition bears some similarity with a recent study of the emergence of rhythmic activity in a network of excitatory cells with spike frequency adaptation (Fuhrmann et al. 2002).

In an interneuron network, ultrafast oscillations (~200 Hz) with the phenomenology of hippocampal ripples during sharp waves can be realized with synaptic time constants similar to those observed in slice studies. The oscillation frequency depends much more on the shortest synaptic time constants (synaptic delay and rise time) than on the synaptic decay time.

In a network composed of both interneurons and excitatory cells, the oscillation is a compromise between two rhythmogenesis scenarios, the purely interneuronal scenario and the pyramidal-to-interneuron loop scenario. The pyramidal-to-interneuron loop scenario involves a much lower frequency (in the gamma range) than the purely interneuronal scenario. Recurrent excitation (both in the E-I and E-E loops) reduces network frequency. The type of oscillation that is generated depends on the relative time scales (τ_E and τ_I) of excitatory and inhibitory synaptic currents and on the balance between the E-I and I-I loops. Networks without pyramidal-to-pyramidal connections can sustain ~200-Hz oscillations when receiving strong external inputs. Interneurons typically lag behind pyramidal cells by ~90° in such networks. Networks with pyramidal-to-pyramidal connections are able to sustain oscillations that are typically in the gamma range (30–100 Hz, depending on the time constants of synapses). When the excitation-inhibition balance is roughly the same in pyramidal cells and interneurons, we predict that there is zero phase difference between the spike discharges of pyramidal and interneuron populations.

Firing-rate synchrony versus spike-to-spike synchrony

The regime of synchronous activity studied in this paper should be contrasted with "spike-to-spike synchrony," which occurs usually without or with weak noise. In networks with spike-to-spike synchrony, the network rhythm arises from synchronization of spikes among neurons that behave as periodic oscillators. Single cells fire a spike at each population cycle or once every few cycles. This kind of synchronization has been studied extensively in the theoretical framework of coupled oscillators (Kopell and Ermentrout 1986; Kuramoto 1984). Many studies have focused on an inhibitory neural network because experimental and theoretical evidence implicates interneurons in the emergence of oscillatory synchrony patterns. In particular, it was found that synchronization depends critically on the synaptic decay time constant (Hansel et al. 1995; Traub et al. 1996; van Vreeswijk et al. 1994; Wang and Buzsáki 1996; Wang and Rinzel 1992; White et al. 1998). Terman et al. (1998) showed that the synaptic rise time also plays a significant role in the synchronization of two mutually inhibitory neurons. There have been some analysis of how synchronization between coupled oscillators depends on the heterogeneity of neuronal properties (Bartos et al. 2001; Hansel and Mato 2003; Neltner et al. 2000; Tiesinga and Jose 2000; Wang and Buzsáki 1996; White et al. 1998) or the sparse random network connectivity (Golomb and Hansel 2000; Wang and Buzsáki 1996). More recently, Hansel and Mato (2001, 2003) considered a two-population model of excitatory and inhibitory neurons as coupled oscillators, where the network is fully connected and without noise. This kind of synchrony is likely to be applicable to networks of pacemaker neurons (regular oscillators), such as in the central pattern generator systems (Marder 1998).

The second type of network synchrony is "firing rate synchrony," which occurs when strong noise and strong inhibitory feedback is present (Brunel 2000; Brunel and Hakim 1999). Here, when a network displays prominent coherent oscillation, spike discharges of single neurons tend to be extremely irregular and intermittent, like a Poisson process with the firing rate much lower than the population oscillation frequency. Fast oscillations in the cortex appears to belong to this category of synchronous activity because spike trains of single cells are usually random and sparse even though the local field potential is rhythmic (Csicsvari et al. 1998; Fries et al 2001). In fact, this type of synchrony is already present in the firing rate models, which were derived under the assumption that single neurons fire spikes stochastically (Wilson and Cowan 1972, 1973).

In a purely interneuronal network, the two types of synchrony produces very different frequency ranges. Networks with spike-to-spike synchrony are typically in the gamma range (Traub et al. 1996; Wang and Buzsáki 1996). We have shown here that networks with firing rate synchrony oscillate at much higher frequencies. Dependency on different synaptic

time scales is another major feature that distinguishes between the two classes of synchronization in an interneuronal network: for spike-to-spike synchrony in oscillator networks, synchrony can appear without any synaptic latency, and the frequency strongly depends on synaptic decay time. For firing-rate synchrony, synchrony depends on a non-zero latency and depends much more weakly on the synaptic decay time. For IPSCs with very short latency and rise times ($\sim$1 ms) and longer decay times ($\sim$5–10 ms), we find that an interneuronal network is able to oscillate at a frequency determined by the fastest time scales (latency and rise times). In this type of oscillation, the decay time affect only weakly the frequency because it is longer than the period of the oscillation.

In a two-population network, the differences between both types of synchrony are less clear cut. Networks tend to oscillate in both cases at frequencies in the gamma range. Phase lags between pyramidal cells and interneurons occur in similar conditions for both types of synchrony (Hansel and Mato 2003). At gamma frequencies, the oscillation becomes sensitively dependent on decay times of both AMPA and GABA currents. Hence, all synaptic time constants potentially play a role in the determination of network frequency.

Comparison with hippocampal oscillations data

In vivo observations indicate that 200 Hz ripples during sharp waves are most prominent in CA1 area, and less reliable in CA3 (Buzsaki et al. 1992; Csicsvari et al. 1999a). Presumably, during sharp waves, CA3 network provides a large excitatory drive, which induces 200-Hz ripples in CA1. On the other hand, 40-Hz (gamma) oscillations appear to be generated within CA3 and propagate to CA1 (Fisahn et al. 1998). Interestingly, CA3 is endowed with an abundance of strong recurrent excitatory connections (Miles and Wong 1986), whereas local collaterals between pyramidal cells are relatively rare and weak in CA1 (Deuchars and Thomson 1996). These observations raise the possibility that the network oscillation frequency (200 vs. 40 Hz) could depend on the strength of intrinsic pyramid-to-pyramid connections. The results shown in this paper are consistent with such a possibility. Interestingly, during sharp wave ripples, CA3 area typically shows variable 100-Hz oscillations (Csicsvari et al. 1999a). The difference in the ripple frequency (100 vs. 200 Hz) between CA3 and CA1 may again be related to the preponderance in CA3, and paucity in CA1, of recurrent excitatory connections.

We have shown that the same network can exhibit different population frequencies, depending on the balance between GABA and AMPA currents. In principle, this balance between excitation and inhibition in the hippocampus can be modulated depending on the behavioral states, for example, by varying differentially the external inputs targetting excitatory and inhibitory cells.

Comparison with neocortical data

Very fast oscillations (from 80 to 600 Hz) have been recently observed in neocortex of anesthetized rats (Jones et al. 2000; Jones and Barth 2002; Kandel and Buzsáki 1997) and cats (Grenier et al. 2001). In these oscillations, single cells typically fire at much lower rates, as in fast oscillations in the hippocampus. Oscillations with frequency $<$200 Hz, as observed in the anesthetized cat (Grenier et al. 2001), seem to be compatible with the scenario discussed in the present paper, in which synaptic inhibition plays a major role. A further indication in favor of the role of inhibition is that neurons recorded with chloride-filled pipettes change their phase relationship with the ripple. On the other hand, the faster (300–500 Hz) oscillations seen by Kandel and Buzsáki (1997) and Jones et al. (2000) seem difficult to reconcile with the present scenario, unless inhibitory time courses are extremely short, and in particular latencies of IPSCs on interneurons are much less than 1 ms (see Fig. 4). Furthermore, Jones and Barth (2002) showed that application of bicuculline does not result in a change of oscillation amplitude or frequency, suggesting a different mechanism is at work in such ultra-fast oscillations.

Model predictions

Our theory has a number of predictions that can be tested experimentally. First, in a noise-dominated inhibitory neural network, the emergence and nature of stochastic fast oscillations depend critically on the synaptic delay of GABAergic connections on interneurons, and in contrast to the coupled oscillator regime, the oscillation frequency is only weakly sensitive to the decay time constant of synaptic inhibition. Second, fast oscillations can be produced either by the interneuronal network or the feedback inhibition in a pyramid-interneuron reciprocal loop. Synchrony in networks with excitatory-inhibitory loops does not necessarily imply a large phase difference in the neural activities of the two cell populations. Pyramidal cells and interneurons can have zero phase difference if recurrent excitatory and inhibitory inputs are balanced in the same way in both cell types. This prediction can be checked in the slice preparation of Fisahn et al. (1998) by measuring the mean excitatory and inhibitory currents in both pyramidal cells and interneurons and comparing the ratios in the two cell types. Third, somewhat contrarily to intuition, inhibition tends to favor very-high-frequency oscillatory patterns, while excitation tends to favor slower oscillatory patterns. Manipulations that alter the balance between recurrent excitation and inhibition can therefore drastically affect network frequency.

Can very fast ($\sim$200 Hz) oscillations be produced by chemical synapses?

Our modeling results suggest that, in principle, very fast oscillations are possible with purely chemical synaptic couplings and no gap junctions. We would like to caution that the present study focused on the effect of synaptic parameters on network frequency and used a simplified (the integrate-and-fire) model of single neurons. This approach allowed us to explore systematically the network behavior in the parameter space. Integrate-and-fire neurons are characterized by a zero neuronal phase lag, for realistic noise models, as was shown by Brunel et al. (2001). This fact allows the network to oscillate at frequencies that are limited only by the speed of synaptic transmission. However, real neurons are endowed with a variety of voltaged-gated ion channels and might differ significantly from the integrate-and-fire model. At least two features of real neurons are not present in integrate-and-fire neurons: subthreshold resonance (see e.g., Hutcheon and Yarom 2000)

and dynamics of ionic channels leading to spike generation. Subthreshold resonances recorded in most neurons appear at rather low frequencies (typically theta), so they should not affect the network dynamics at the high frequencies considered here. On the other hand, dynamics of ionic channels leading to spike generation could in principle affect the high-frequency neuronal response. In a companion paper (C. Geisler, N. Brunel, and X.-J. Wang, unpublished observations), the contribution of intrinsic cellular dynamics to the oscillation frequency and network synchronization is investigated extensively. In particular, we find that with Hodgkin-Huxley-type conductance-based neurons, instead of the integrate-and-fire neurons, very-high-frequency (200 Hz) oscillations can be achieved (Geisler, et al., unpublished observations) provided that certain assumptions are satisfied, for example, when the effective membrane time constants of the neurons are small enough.

Furthermore, even if the chemical synapse mechanism is sufficient to produce 200-Hz oscillations under some conditions, it does not rule out other scenarios for the generation of very fast oscillations, such as axo-axonic gap junctions between pyramidal cells (Lewis and Rinzel 2000; Schmitz et al. 2001; Traub et al. 1999; Traub and Bibbig 2000). In some systems, very fast oscillations are not suppressed by GABAergic antagonists (Draguhn et al. 1998; Jones and Barth 2002), leaving gap junctions as the leading alternative mechanism. In other systems, such that the hippocampus of a freely moving rat, whether chemical, electrical, or both, connections are needed remains an open question.

Further experimental and theoretical work will be necessary to obtain a general framework for understanding synchronous network rhythms characterized by irregular neuronal spike discharges and help to resolve the well-known dichotomy between oscillatory local field potential of a cortical circuit and the highly stochastic spike trains of its constituent neurons (Engel et al. 1992; Fries et al. 2001).

APPENDIX 1. NETWORKS WITH E-I CONNECTION ONLY

Here, we repeat the analysis of the purely interneuronal network (steps 1–4 in RESULTS) for a network with connections between pyramidal cells and interneurons but no connections between pyramidal cells, or between interneurons.

Step 1

In the excitatory-inhibitory network, we look for solutions of network activity of the form

$$\nu_E(t) = \nu_{E,0}[1 + \epsilon_E \exp(i\omega t)] \tag{A1}$$

$$\nu_I(t) = \nu_{I,0}[1 + \epsilon_I \exp(i\omega t)] \tag{A2}$$

where $\nu_{E,0}$ and $\nu_{I,0}$ are the average firing rates, ϵ_E and ϵ_I are the relative strengths of the deviations to the stationary firing rates (including a possible phase lag between the two populations).

Step 2

The GABAergic synaptic variable is given by *Eq. 6.* The AMPA synapses are described by

$$s_E = s_{E,0}[1 + \epsilon_E S_E(\omega) \exp(i\omega t - i\Phi_E(\omega))] + \text{noise} \tag{A3}$$

where $s_{E,0}$ is the average fraction of open channels at AMPA synapses, summed over all synapses,

$$S_E(\omega) = \frac{1}{\sqrt{(1 + \omega^2\tau_{dE}^2)(1 + \omega^2\tau_{rE}^2)}}$$

is the attenuation in the amplitude of the oscillation induced by AMPA current dynamics, and

$$\Phi_E(\omega) = \omega\tau_{IE} + \text{atan}\,(\omega\tau_{rE}) + \text{atan}\,(\omega\tau_{dE})$$

is the phase lag introduced by AMPA current filtering.

The recurrent synaptic currents are

$$I_{AMPA\to I} = I_{AMPA\to I,0}[1 + \epsilon_E S_E \exp(i\omega t - i\Phi_E(\omega))] + \text{noise} \tag{A4}$$

$$I_{GABA\to E} = I_{GABA\to E,0}[1 + \epsilon_I S_I \exp(i\omega t - i\Phi_I(\omega))] + \text{noise} \tag{A5}$$

The total synaptic currents on pyramidal cells and interneurons are

$$I_{syn\to I} = I_{syn\to I,0}\left[1 + \epsilon_E S_E \frac{I_{AMPA\to I,0}}{I_{syn\to I,0}} \exp(i\omega t - i\Phi_E(\omega))\right] + \text{noise} \tag{A6}$$

$$I_{syn\to E} = I_{syn\to E,0}\left[1 + \epsilon_I S_I \frac{I_{GABA\to E,0}}{I_{syn\to E,0}} \exp(i\omega t + i\pi - i\Phi_I(\omega))\right] + \text{noise} \tag{A7}$$

Step 3

The firing rate of pyramidal cells and interneurons are

$$\nu_E(t) = \nu_{E,0}\left[1 + \epsilon_I S_I \frac{I_{GABA\to E,0}}{I_{syn\to E,0}} A_E \exp(i\omega t + i\pi - i\Phi_I(\omega))\right]$$

$$\nu_I(t) = \nu_{I,0}\left[1 + \epsilon_E S_E \frac{I_{AMPA\to I,0}}{I_{syn\to I,0}} A_I \exp(i\omega t - i\Phi_E(\omega))\right]$$

where A_E measures the relative change in firing rate induced by a relative change in average input current, $A_E = I_{syn\to E,0}/\nu_{E,0}\partial\nu_{E,0}(I_{syn\to E,0})/\partial I_{syn\to E,0}$.

Step 4

Steps 3 and 1 imply that the oscillatory components in pyramidal cell activity and interneuron oscillatory activity are related by

$$\epsilon_E = \epsilon_I S_I \frac{I_{GABA\to E,0}}{I_{syn\to E,0}} A_E \exp(i\pi - i\Phi_I(\omega)) \tag{A8}$$

$$\epsilon_I = \epsilon_E S_E \frac{I_{AMPA\to I,0}}{I_{syn\to I,0}} A_I \exp(-i\Phi_E(\omega)) \tag{A9}$$

Solving these two equations yields the phase condition

$$\pi = \Phi_E(\omega) + \Phi_I(\omega)$$

which determines the oscillation frequency ω (or $f = \omega/(2\pi)$). Note that, by our convention, interneurons lag excitatory cells by $\Phi_E(\omega)$.

APPENDIX 2. NETWORKS WITH E-I AND I-I LOOPS

When the I-I connections are added, we can still use *Eqs. A1* and *A2* for the firing rates of the two cell types, but now the interneurons receive an additional (inhibitory) synaptic current. Therefore the total synaptic currents on pyramidal cells and interneurons become

$$I_{syn\to E} = I_{syn\to E,0}\left[1 + \epsilon_I S_I \frac{I_{GABA\to E,0}}{I_{syn\to E,0}} \exp(i\omega t + i\pi - i\Phi_I(\omega))\right] + \text{noise} \tag{B1}$$

$$I_{syn\to I} = I_{syn\to I,0}\left[1 + \epsilon_E S_E \frac{I_{AMPA\to I,0}}{I_{syn\to I,0}} \exp(i\omega t - i\Phi_E(\omega)) \right. \tag{B2}$$

$$+ \epsilon_I S_I \frac{I_{GABA\to I,0}}{I_{syn\to I,0}} \exp(i\omega t + i\pi - i\Phi_I(\omega)) + \text{noise} \quad (B3)$$

The firing rate of pyramidal cells and interneurons are

$$\nu_E(t) = \nu_{E,0}[1 + \epsilon_I X_{EI} \exp(i\omega t + i\pi - i\Phi_I(\omega)]$$

$$\nu_I(t) = \nu_{I,0}[1 + \epsilon_E X_{IE} \exp(i\omega t - i\Phi_E(\omega)) + \epsilon_I X_{II} \exp(i\omega t + i\pi - i\Phi_I(\omega))]$$

where the parameters X_{EI}, X_{IE} and X_{II} measure the relative attenuation introduced by the corresponding types of connections,

$$X_{EI} = S_I \frac{I_{GABA\to E,0}}{I_{syn\to E,0}} A_E \quad (B4)$$

$$X_{IE} = S_E \frac{I_{AMPA\to I,0}}{I_{syn\to I,0}} A_I \quad (B5)$$

$$X_{II} = S_I \frac{I_{GABA\to I,0}}{I_{syn\to I,0}} A_I \quad (B6)$$

The parameters X_{EI}, X_{IE}, and X_{II} are proportional to the strengths of the corresponding types of connections (inhibitory synapses on pyramidal cells, excitatory and inhibitory synapses on inhibitory cells, respectively) through their dependency on the mean currents $I_{GABA\to E,0}$, $I_{AMPA\to I,0}$, and $I_{GABA\to I,0}$.

Equalizing the rates in *Eq. B4* and in *Eq. A1*, it is clear that the oscillatory components in pyramidal cell activity and interneuron oscillatory activity are related by

$$\epsilon_E = \epsilon_I X_{EI} \exp(i\pi - i\Phi_I(\omega)) \quad (B7)$$

$$\epsilon_I = \epsilon_E X_{IE} \exp(-i\Phi_E(\omega)) + \epsilon_I X_{II} \exp(i\pi - i\Phi_I(\omega)) \quad (B8)$$

Solving *Eqs. (B8)* yields the phase condition

$$\pi = \Phi_I(\omega) + \text{atan}\left(\frac{(X_{IE}X_{EI}/X_{II}) \sin(\Phi_E(\omega))}{(X_{IE}X_{EI}/X_{II}) \cos(\Phi_E(\omega)) + 1}\right) \quad (B9)$$

which determines the oscillation frequency. Thus the additional phase lag due to the E-I loop is weighted by the relative weight between the E-I loop and the I-I loop, as measured by the parameter $(X_{IE}X_{EI}/X_{II})$.

The phase lag between interneurons and pyramidal cells is

$$\text{atan}\left(\frac{(X_{IE}X_{EI}/X_{II}) \sin(\Phi_E(\omega))}{(X_{IE}X_{EI}/X_{II}) \cos(\Phi_E(\omega)) + 1}\right) \quad (B10)$$

APPENDIX 3. NETWORKS WITH E-E, E-I, AND I-I LOOPS

It is straightforward to repeat the analysis with the addition of E-E connections. The resulting relationships between excitatory and inhibitory activities are

$$\epsilon_E = \epsilon_E X_{EE} \exp(-i\Phi_E(\omega)) + \epsilon_I X_{EI} \exp(i\pi - i\Phi_I(\omega)) \quad (C1)$$

$$\epsilon_I = \epsilon_E X_{IE} \exp(-i\Phi_E(\omega)) + \epsilon_I X_{II} \exp(i\pi - i\Phi_I(\omega)) \quad (C2)$$

with

$$X_{EE} = S_E \frac{I_{AMPA\to E,0}}{I_{syn\to E,0}} A_E$$

yielding

$$1 = X_{EE} \exp(-i\Phi_E(\omega)) + X_{II} \exp(i\pi - i\Phi_I(\omega)) + (X_{EI}X_{IE} - X_{EE}X_{II}) \exp(i\pi - i\Phi_I(\omega) - i\Phi_E(\omega)) \quad (C3)$$

from which the phase condition can be deduced. Note that when only E-E connections are present, the phase condition becomes $\Phi_E(\omega) = 0$ whose solution is $\omega = 0$.

When the balance between excitation and inhibition is the same in pyramidal cells and interneurons

$$\frac{X_{EE}}{X_{EI}} = \frac{X_{IE}}{X_{II}} = \frac{S_E I_{AMPA}}{S_I I_{GABA}}$$

Under this condition, the last term in *Eq. C3* is zero, and the equation simplifies to

$$1 = X_{EE} \exp(-i\Phi_E(\omega)) + X_{II} \exp(i\pi - i\Phi_I(\omega)) \quad (C4)$$

If we further assume $A_E = A_I$, *Eq. C4* gives the set of two equations

$$1 = X_{II}\left(-\cos\Phi_I(\omega) + \frac{S_E(\omega) I_{AMPA}}{S_I(\omega) I_{GABA}} \cos\Phi_E(\omega)\right) \quad (C5)$$

$$0 = \sin\Phi_I(\omega) - \frac{S_E(\omega) I_{AMPA}}{S_I(\omega) I_{GABA}} \sin(\Phi_E(\omega)) \quad (C6)$$

where the second equation *C6* is the phase condition that determines the oscillation frequency, while the first equation *C5* determines the location of the onset of the oscillations in parameter space. *Eq. C6* shows that the frequency depends both on the synaptic time constants, through the synaptic variables Φ_E, Φ_I, S_E, and S_I and on the balance between recurrent excitation and inhibition, I_{AMPA}/I_{GABA}. Combining *Eq. C4* with *Eq. C2*, we find that $\epsilon_E = \epsilon_I$. In other words, there is zero phase lag between pyramidal cells and interneurons.

Solving numerically *Eq. C6*, we find that when excitatory time constants are shorter or equal to inhibitory time constants, excitation *decreases* monotonically the oscillation frequency. The condition for this to happen is $\sin(\Phi_E(\omega_I)) > 0$, where ω_I is the network frequency for a purely inhibitory network. When excitation time constants are long enough, resulting in $\sin(\Phi_E(\omega_I)) < 0$, excitation increases the oscillation frequency for small values of the ratio I_{AMPA}/I_{GABA}. This phenomenon is investigated in more detail in Geisler (unpublished observations).

N. Brunel thanks the Volen Center, where this work was initiated, for its hospitality and is indebted to D. Hansel for discussions about synchrony in recurrent networks and comments on the manuscript. X. J. Wang thanks the hospitality of Ecole Normale Supérieure, where this work was partly carried out.

X. J. Wang was supported by the National Institute of Mental Health Grant MH-62349, the Alfred P. Sloan Foundation, and the Swartz Foundation.

REFERENCES

Abbott LF and van Vreeswijk C. Asynchronous states in a network of pulse-coupled oscillators. *Phys Rev E* 48: 1483–1490, 1993.

Angulo MC, Rossier J, and Audinat E. Postsynaptic glutamate receptors and integrative properties of fast-spiking interneurons in the rat neocortex. *J Neurophysiol* 82: 1295–1302, 1999.

Bartos M, Vida I, Frotscher M, Geiger JRP, and Jonas P. Rapid signaling at inhibitory synapses in a dendate gyrus interneuron network. *J Neurosci* 21: 2687–2698, 2001.

Bartos M, Vida I, Frotscher M, Meyer A, Monyer H, Geiger JRP, and Jonas P. Fast synaptic inhibition promotes synchronized gamma oscillations in hippocampal interneuron networks. *Proc Natl Acad Sci USA* 99: 13222–13227, 2002.

Bragin A, Jando G, Nadasdy Z, Hetke J, Wise K, and Buzsáki G. Gamma (40–100 Hz) oscillation in the hippocampus of the behaving rat. *J Neurosci* 15: 47–60, 1995.

Brunel N. Dynamics of sparsely connected networks of excitatory and inhibitory spiking neurons. *J Comput Neurosci* 8: 183–208, 2000.

Brunel N, Chance F, Fourcaud N, and Abbott L. Effects of synaptic noise and filtering on the frequency response of spiking neurons. *Phys Rev Lett* 86: 2186–2189, 2001.

Brunel N and Hakim V. Fast global oscillations in networks of integrate-and-fire neurons with low firing rates. *Neural Comput* 11: 1621–1671, 1999.

Buhl DL, Harris KD, Hormuzd SG, Monyer H, and Buzsáki G. Selective impairment of hippocampal gamma oscillations in connexin-36 knock-out mouse in vivo. *J. Neurosci* 23: 1013–1018, 2003

Buhl EH, Tamas G, and Fisahn A. Cholinergic activation and tonic excitation induce persistent gamma oscillations in mouse somatosensory cortex in vitro. *J Physiol* 513: 117–126, 1998.

Buhl EH, Tamas G, Szilagyi T, Stricker C, Paulsen O, and Somogyi P. Effect, number, and location of synapses made by single pyramidal cells onto aspiny interneurons of cat visual cortex. *J Physiol* 500: 689–713, 1997.

Buzsaki G, Urioste R, Hetke J, and Wise K. High-frequency network oscillation in the hippocampus. *Science* 256: 1025–1027, 1992.

Csicsvari J, Hirase H, Czurko A, and Buzsáki G. Reliability and state dependence of pyramidal cell-interneuron synapses in the hippocampus: an ensemble approach in the behaving rat. *Neuron* 21: 179–189, 1998.

Csicsvari J, Hirase H, Czurko A, Mamiya A, and Buzsáki G. Fast network oscillations in the hippocampal ca1 region of the behaving rat. *J Neurosci* 19: RC20, 1999a.

Csicsvari J, Hirase H, Czurko A, Mamiya A, and Buzsáki G. Oscillatory coupling of hippocampal pyramidal cells and interneurons in the behaving rat. *J Neurosci* 19: 274–287, 1999b.

Deuchars J and Thomson AM. CA1 pyramid-pyramid connections in rat hippocampus in vitro: dual intracellular recordings with biocytin filling. *Neuroscience* 74: 1009–1018, 1996.

Draguhn A, Traub RD, Schmitz D, and Jefferys JGR. Electrical coupling underlies high-frequency oscillations in the hippocampus in vitro. *Nature* 394: 189–193, 1998.

Engel AK, Konig TBSP, Kreiter AK, and Singer WR. Temporal coding in the visual cortex: new vistas on integration in the nervous system. *Trends Neurosci* 15: 218–226, 1992.

Fellous J and Sejnowski TJ. Cholinergic induction of oscillations in the hippocampal slice in the slow (0.5–2 Hz), theta (5–12 Hz) and gamma bands. *Hippocampus* 10: 187–197, 2000.

Fisahn A, Pike FG, Buhl EH, and Paulsen O. Cholinergic induction of network oscillations at 40 hz in the hippocampus in vitro. *Nature* 394: 186–189, 1998.

Fourcaud N and Brunel N. Dynamics of firing probability of noisy integrate-and-fire neurons. *Neural Comput* 14: 2057–2110, 2002.

Freeman WJ. *Mass Action in the Nervous System.* New York: Academic Press, 1975.

Fries P, Reynolds JH, Rorie AE, and Desimone R. Modulation of oscillatory neuronal synchronization by selective visual attention. *Science* 291: 1560–1563, 2001.

Fuhrmann G, Markram H, and Tsodyks M. Spike frequency adaptation and neocortical rhythms. *J Neurophysiol* 88: 761–770, 2002.

Gerstner W. Time structure of the activity in neural network models. *Phys Rev E* 51: 738–758, 1995.

Gerstner W, van Hemmen L, and Cowan J. What matters in neuronal locking? *Neural Comput* 8: 1653–1676, 1996.

Golomb D and Hansel D. The number of synaptic inputs and the synchrony of large sparse neuronal networks. *Neural Comput* 12: 1095–1139, 2000.

Golomb D and Rinzel J. Clustering in globally coupled inhibitory neurons. *Physica D* 72: 259–282, 1994.

Grenier F, Timofeev I, and Steriade M. Focal synchronization of ripples (80–200 Hz) in neocortex and their neuronal correlates. *J Neurophysiol* 86: 1884–1898, 2001.

Gupta A, Wang Y, and Markram H. Organizing principles for a diversity of GABAergic interneurons and synapses in the neocortex. *Science* 287: 273–278, 2000.

Hansel D and Mato G. Existence and stability of persistent states in large neuronal networks. *Phys Rev Lett* 10: 4175–4178, 2001.

Hansel D and Mato G. Asynchronous states and the emergence of synchrony in large networks of interacting excitatory and inhibitory neurons. *Neural Comput* 15: 1–56, 2003.

Hansel D, Mato G, and Meunier C. Synchrony in excitatory neural networks. *Neural Comput* 7: 307–337, 1995.

Hansel D, Mato G, Meunier C, and Neltner L. On numerical simulations of integrate-and-fire neural networks. *Neural Comput* 10: 467–483, 1998.

Hansel D and Sompolinsky H. Chaos and synchrony in a model of a hypercolumn in visual cortex. *J Comput Neurosci* 3: 7–34, 1996.

Hestrin S, Sah P, and Nicoll R. Mechanisms generating the time course of dual component excitatory synaptic currents recorded in hippocampal slices. *Neuron* 5: 247–253, 1990.

Hormuzdi SG, Pais I, LeBeau FE, Towers SK, Rozov A, Buhl EH, Whittington MA, and Monyer H. Impaired electrical signaling disrupts gamma frequency oscillations in connexin 36-deficient mice. *Neuron* 31: 487–495, 2001.

Hutcheon B and Yarom Y. Resonance, oscillation and the intrinsic frequency preferences of neurons. *Trends Neurosci* 23: 216–222, 2000.

Jefferys JG, Traub RT, and Whittington MA. Neuronal networks for induced "40-Hz" rhythms. *Trends Neurosci* 19: 202–208, 1996.

Jones MS and Barth DS. Effects of bicuculline methiodide on fast (>200 Hz) electrical oscillations in rat somatosensory cortex. *J Neurophysiol* 88: 1016–1025, 2002.

Jones MS, MacDonald KD, Chol B, Dudek E, and Barth DS. Intracellular correlates of fast (>200 Hz) electrical oscillations in rat somatosensory cortex. *J Neurophysiol* 84: 1505–1518, 2000.

Kandel A and Buzsáki G. Cellular-synaptic generation of sleep spindles, spike-and-wave discharges, and evoked thalamocortical responses in the neocortex of the rat. *J Neurosci* 17: 6783–6797, 1997.

Kopell N and Ermentrout GB. Symmetry and phaselocking in chains of weakly coupled oscillators. *Comm Pure Appl Math* 39: 623–660, 1986.

Kopell N and LeMasson G. Rhythmogenesis, amplitude modulation, and multiplexing in a cortical architecture. *Proc Natl Acad Sci USA* 91: 10586–10590, 1994.

Kraushaar U and Jonas P. Efficacy and stability of quantal GABA release at a hippocampal interneuron-principal neuron synapse. *J Neurosci* 20: 5594–5607, 2000.

Kuramoto Y. *Chemical Oscillations, Waves and Turbulence.* New York: Springer-Verlag, 1984.

Leung LS. Nonlinear feedback model of neuronal populations in hippocampal CA1 region. *J Neurophysiol* 47: 845–868, 1982.

Lewis TJ and Rinzel J. Self-organized synchronous oscillations in a network of excitable cells coupled by gap junctions. *Network* 11: 299–320, 2000.

Logothetis NK, Pauls J, Augath MA, Trinath T, and Oeltermann A. Neurophysiological investigation of the basis of the fMRI signal. *Nature* 412: 150–157, 2001.

Marder E. From biophysics to models of network function. *Annu Rev Neurosci* 21: 25–45, 1998.

Markram H, Lubke J, Frotscher M, Roth A, and Sakmann B. Physiology and anatomy of synaptic connections between thick tufted pyramidal neurones in the developing rat neocortex. *J Physiol (London)* 500: 409–440, 1997.

Miles R and Wong RK. Excitatory synaptic interactions between ca3 neurones in the guinea pig hippocampus. *J Physiol* 373: 397–418, 1986.

Neltner L, Hansel D, Mato G, and Meunier C. Synchrony in heterogeneous neural networks. *Neural Comp* 12: 1607–1641, 2000.

Press WH, Teukolsky SA, Vetterling WT, and Flannery BP. *Numerical Recipes in C.* Cambridge, UK: Cambridge Univ. Press, 1992.

Salin PA and Prince DA. Spontaneous $GABA_A$ receptor mediated inhibitory currents in adult rat somatosensory cortex. *J Neurophysiol* 75: 1573–1588, 1996.

Schmitz D, Schuchmann S, Fisahn A, Draguhn A, Buhl EH, Petrasch-Parwez W, Dermietzel R, Heinemann U, and Traub RD. Axo-axonal coupling a novel mechanism for ultrafast neuronal communication. *Neuron* 31: 831–840, 2001.

Shelley MJ and Tao L. Efficient and accurate time-stepping schemes for integrate-and-fire neuronal networks. *J Comput Neurosci* 11: 111–119, 2001.

Siapas AG and Wilson MA. Coordinated interactions between hippocampal ripples and cortical spindles during slow-wave sleep. *Neuron* 21: 1123–1128, 1998.

Tamas G, Buhl EH, and Somogyi P. Fast IPSPs elicited via multiple synaptic release sites by different types of GABAergic neurons in the cat visual cortex. *J Physiol* 500: 715–738, 1997.

Tamas G, Somogyi P, and Buhl EH. Differentially interconnected networks of GABAergic interneurons in the visual cortex of the cat. *J Neurosci* 18: 4255–4270, 1998.

Tegnér J, Compte A, and Wang X-J. Dynamical stability of hebbian reverberatory neural networks. *Biol Cybern* 87: 471–481, 2002.

Terman D, Kopell N, and Bose A. Dynamics of two mutually coupled slow inhibitory neurons. *Physica D* 117: 241–275, 1998.

Tiesinga PH and Jose JV. Robust gamma oscillations in networks of inhibitory hippocampal interneurons. *Network* 11: 1–23, 2000.

Traub RD and Bibbig A. A model of high-frequency ripples in the hippocampus based on synaptic coupling plus axon-axon gap junctions between pyramidal neurons. *J Neurosci* 20: 2086–2093, 2000.

Traub RD, Schmitz D, Jefferys JGR, and Draguhn A. High-frequency population oscillations are predicted to occur in hippocampal pyramidal neuronal networks interconnected by axoaxonal gap junctions. *Neuroscience* 92: 407–426, 1999.

Traub RD, Whittington MA, Collins SB, Buzsáki G, and Jefferys JGR. Analysis of gamma rhythms in the rat hippocampus in vitro and in vivo. *J Physiol* 493: 471–484, 1996.

Treves A. Mean-field analysis of neuronal spike dynamics. *Network* 4: 259–284, 1993.

Tsodyks MV, Skaggs WE, Sejnowski TJ, and McNaughton BL. Paradoxical effects of external modulation of inhibitory interneurons. *J Neurosci* 17: 4382–4388, 1997.

Tuckwell HC. *Introduction to Theoretical Neurobiology.* Cambridge, UK: Cambridge Univ. Press, 1988.

van Vreeswijk C, Abbott L, and Ermentrout GB. When inhibition not excitation synchronizes neural firing. *J Comput Neurosci* 1: 313–321, 1994.

van Vreeswijk C and Sompolinsky H. Chaos in neuronal networks with balanced excitatory and inhibitory activity. *Science* 274: 1724–1726, 1996.

Vida I, Halasy K, Szinyei C, Somogyi P, and Buhl EH. Unitary IPSPs evoked by interneurons at the stratum radiatum-stratum lacunosum-molecolare border in the CA1 area of the rat hippocampus in vitro. *J Physiol* 506: 755–773, 1998.

Wang X-J. Synaptic basis of cortical persistent activity: the importance of NMDA receptors to working memory. *J Neurosci* 19: 9587–9603, 1999.

Wang X-J and Buzsáki G. Gamma oscillation by synaptic inhibition in a hippocampal interneuronal network model. *J Neurosci* 16: 6402–6413, 1996.

Wang X-J, Golomb D, and Rinzel J. Emergent spindle oscillations and intermittent burst firing in a thalamic model: specific neuronal mechanisms. *Proc Natl Acad Sci USA* 92: 5577–5581, 1995.

Wang X-J and Rinzel J. Alternating and synchronous rhythms in reciprocally inhibitory model neurons. *Neural Comput* 4: 84–97, 1992.

White JA, Chow CC, Soto-Treviño C, and Kopell N. Synchronization and oscillatory dynamics in heterogeneous, mutually inhibited neurons. *J Comput Neurosci* 5: 5–16, 1998.

Wilson HR and Cowan JD. Excitatory and inhibitory interactions in localized populations of model neurons. *Biophys J* 12: 1–24, 1972.

Wilson HR and Cowan JD. A mathematical theory of the functional dynamics of cortical and thalamic nervous tissue. *Kybernetik* 13: 55–80, 1973.

Xiang Z, Huguenard JR, and Prince DA. $GABA_A$ receptor mediated currents in interneurons and pyramidal cells of rat visual cortex. *J Physiol* 506: 715–730, 1998.

Zhou F-M and Hablitz JJ. AMPA receptor-mediated EPSCs in rat neocortical layer II/III interneurons have rapid kinetics. *Brain Res* 780: 166–169, 1998.